Technical Report Documentation Page

1. Report No.	2. Government Accession No.	3. Recipient's Catalog No.
FHWA/TX-11/0-6100-3		

4. Title and Subtitle	5. Report Date
DEVELOPMENT OF PRECAST BRIDGE DECK OVERHANG SYSTEM: TECHNICAL REPORT	February 2010 Publish: July 2011
	6. Performing Organization Code
7. Author(s)	8. Performing Organization Report No.
David Trejo and Young Hoon Kim	Report 0-6100-3
9. Performing Organization Name and Address	10. Work Unit No. (TRAIS)
Texas Transportation Institute The Texas A&M University System College Station, Texas 77843-3135	11. Contract or Grant No. Project 0-6100
12. Sponsoring Agency Name and Address	13. Type of Report and Period Covered
Texas Department of Transportation Research and Technology Implementation Office P. O. Box 5080 Austin, Texas 78763-5080	Technical Report: September 2007–August 2009
	14. Sponsoring Agency Code

15. Supplementary Notes

Project performed in cooperation with the Texas Department of Transportation and the Federal Highway Administration.
Project Title: Development of Precast Bridge Deck Overhang System
URL: http://tti.tamu.edu/documents/0-6100-3.pdf

16. Abstract

The implementation of full-depth, precast overhang panel systems has the potential to improve constructability, productivity, and make bridges more economical. Initial testing and analyses reported in the 0-6100-2 report resulted in a design that required a large number of shear pockets in the overhang panels. The general design methodology used in this report was to determine the number of connectors based on the shear capacity of a girder with conventional R-bars (not necessarily based on the required demand). The large number of shear pockets reduced the constructability and economy of the precast overhang system. Report 0-6100-1 (produced after 0-6100-2) used the American Association of State Highway Officials Load and Resistance Factor Design (AASHTO LRFD [2008]) demand requirements to design the number of shear pockets for a precast overhang panel system and reported that the number of pockets per panel could be reduced from the numbers reported in report 0-6100-2. However, this report only included an analysis for one beam type and one span length. In addition, the demand load used did not include all factors typically used by designers. Additional testing was required to assess different connector systems and further analyses were needed for the new Texas Department of Transportation (TxDOT) girders. The testing and analyses documented in this report (0-6100-3) provides a new equation for determining the number of shear pockets required for the various shear connector/coupler systems evaluated in this research. This equation was used to determine the number of shear pockets required for the newer TxDOT girders. Results from this research indicate that the roughened surface provides strong adhesion between the top girder surface and a precast panel. Steel reinforcing hoops placed in the shear pocket and shear reinforcing hoops placed in the overhang panel around the opening of the shear pocket provided limited or no improvement in capacity of the shear connector/coupler system. Hollow structural section (HSS) steel tubes placed around the perimeter of the shear pocket during fabrication did result in samples with higher shear capacities and could result in overhang panels with fewer shear pockets. This system could make constructing bridges with precast overhang systems more constructible, economical, and could reduce the construction time.

17. Key Words	18. Distribution Statement
Shear Friction, Push-Off Test, Composite System, Anchor Type	No restrictions. This document is available to the public through NTIS: National Technical Information Service Alexandria, Virginia 22312 http://www.ntis.gov

19. Security Classif.(of this report)	20. Security Classif.(of this page)	21. No. of Pages	22. Price
Unclassified	Unclassified	60	

Form DOT F 1700.7 (8-72) **Reproduction of completed page authorized**

DEVELOPMENT OF PRECAST BRIDGE DECK OVERHANG SYSTEM: TECHNICAL REPORT

by

David Trejo, Ph.D., P.E.
Professor and Hal D. Pritchett Endowed Chair

and

Young Hoon Kim, Ph.D.
Post-Doctoral Scholar

School of Civil and Construction Engineering
Oregon State University
(formerly at the Texas Transportation Institute)

Report 0-6100-3
Project 0-6100
Project Title: Development of Precast Bridge Deck Overhang System

Performed in cooperation with the
Texas Department of Transportation
and the
Federal Highway Administration

February 2010
Publish: July 2011

TEXAS TRANSPORTATION INSTITUTE
The Texas A&M University System
College Station, Texas 77843-3135

DISCLAIMER

The contents of this report reflect the views of the authors, who are responsible for the facts and the accuracy of the data presented herein. The contents do not necessarily reflect the official view or policies of the Federal Highway Administration (FHWA) or the Texas Department of Transportation (TxDOT). This report does not constitute a standard, specification, or regulation. The engineer in charge was David Trejo, Ph.D., P.E. #93490.

The United States Government and the State of Texas do not endorse products or manufacturers. Trade or manufacturers' names appear herein solely because they are considered essential to the objective of this report.

ACKNOWLEDGMENTS

This project was conducted at Texas A&M University (TAMU) and was supported by TxDOT and FHWA through the Texas Transportation Institute (TTI) as part of Project 0-6100, Development of Precast Bridge Deck Overhang System. The valuable input of Dr. German Claros, Mr. Ricardo Gonzalez, Mr. Ralph Browne, Mr. Graham Bettis, Mr. Manuel Padron, Mr. Alfredo Valles, Mr. John Holt, Mr. Loyl Bussell, Mr. Robert Cochrane, Mr. Lewis Gamboa, Mr. Michael Hyzak, and Mr. Brian Merrill is appreciated. The authors also wish to thank Dr. Peter Keating, Mr. Matt Potter of the Civil Engineering High Bay Structural and Materials Laboratory (HBSML) at TAMU; and Dr. Radhakrishna Pillai for their continuous support and assistance, and all the students who assisted with the project.

TABLE OF CONTENTS

Page

LIST OF FIGURES

LIST OF TABLES

1. INTRODUCTION

1.1. GENERAL

Precast girders and precast deck panels have been used widely in bridge construction. Figure 1-1 shows a portion of a bridge made of precast girder and precast deck systems.

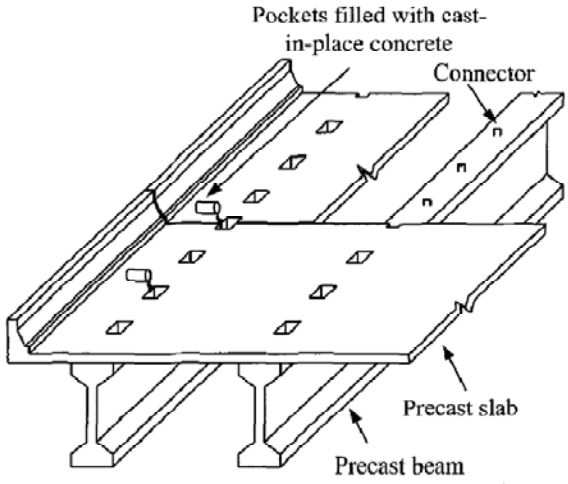

Figure 1-1. Precast girder and deck system (Araujo and Debs 2005)

In this report, a shear connector is defined as a system that connects the girder and deck panels. As shown in Figure 1-1, a typical shear connector system consists of steel connectors (made of conventional reinforcement hooks known as R-bars) provided across the girder and the shear pockets in the deck panels. These shear pockets are then typically filled with cementitious grout or cast-in-place (CIP) concrete. This system assists in achieving a composite action between the precast girders and precast deck panels on a bridge.

Over the last few decades there have been several studies investigating the horizontal shear mechanism between the precast girders and precast deck panels. As precast systems become more common, there is a need to identify systems that have the potential to reduce construction time and increase safety at the time of construction. Reports on the previous phases

of this project (0-6100-1 and 0-6100-2) indicated that the shear capacity of the shear connectors between the girder and full-depth overhang panels was low and recommended panels with a larger number of shear pockets. However, providing more shear pockets increases construction costs and reduces the constructability. Therefore, research is needed to improve the performance of shear connectors for precast overhang systems.

1.2. OBJECTIVES

For precast girder and precast overhang deck systems, it is important not only to align and place the precast deck panels at the correct position on the girder, but also to connect each other to achieve composite action. Early research results indicated low shear capacity in the shear connector systems and therefore, the capacity of the shear connector system requires further investigation. The objectives of this research are to:

- investigate the efficiency of eight types of shear connectors between girders and full-depth overhang panels and
- develop and recommend an improved shear connector design with reduced number of shear pockets and maximized shear capacity per shear pocket.

To achieve these objectives, the shear strength and behavior of eight different types of connector systems with triplicate specimens for each system type (i.e., a total of 24 tests) were fabricated, tested, and assessed.

1.3. ORGANIZATION OF THIS REPORT

Section 2 provides a brief review of previous studies related to shear friction in concrete systems and the design equations based on shear friction and push-off tests. Section 3 presents the overall experimental program, which covers test matrix, test procedures, and the design or layout of test samples. This section also provides properties of the materials used in this research. Section 4 discusses the test results and the design methods to estimate the optimum number of pockets for the precast panels. Finally, the findings from this project and recommendations are summarized in Section 5.

2. LITERATURE REVIEW

2.1. GENERAL

Research has been conducted to better understand the behavior of shear connectors in precast deck systems (Scholz et al. 2007, National Cooperative Highway Research Program [NCHRP] 584 2008). Shear friction on cast-in-place CIP deck systems has been studied and many equations have been recommended (AASHTO LRFD 2007LRFD 2007).

2.2. SHEAR FRICTION THEORY

Birkeland and Birkeland (1966) proposed the simple physical model for shear friction. Figure 2-1 shows the shear-friction hypothesis.

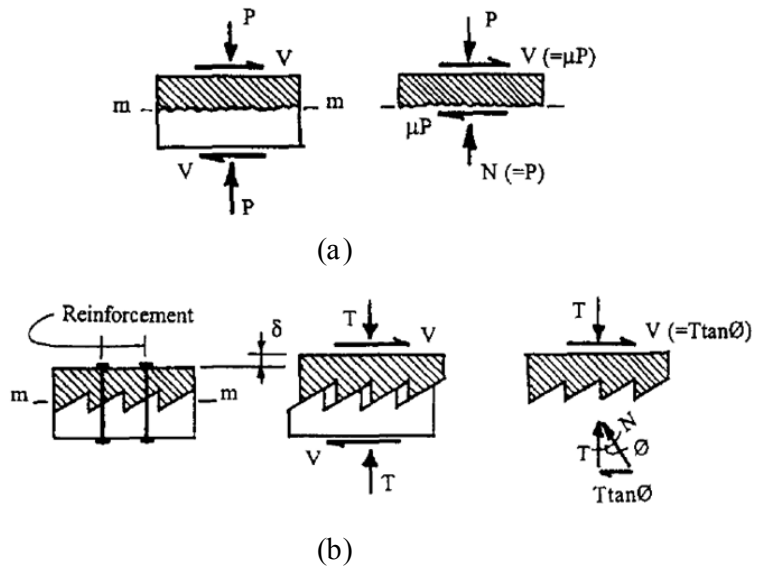

Figure 2-1. Shear-friction hypothesis (Birkeland and Birkeland 1966)

As shown in Figure 2-1(a), consider a case with no shear connector across the shear plane. For an element to slide along the assumed shear plane, *m-m*, the shear force, *V*, should be

increased up to μP, where μ is coefficient of friction and P is the normal force. Now, consider the case with a shear connector, as shown in Figure 2-1(b). As the slip progresses, a normal displacement, δ, occurs. This displacement can be large enough to cause yielding of the shear connector. Also, this displacement induces a tension force, T, in the shear connector placed across the roughened shear plane. This tension force is equal to the clamping force and is calculated as follows:

$$T = A_{vf} f_y \tag{2.1}$$

where A_{vf} and f_y are the cross-sectional area and yield strength of the shear connector. The sawtooth in Figure 2-1(b) represents the surface roughness, which assists in resisting the shear force, V. The term V can be calculated as follows:

$$V = T \tan \phi = A_{vf} f_y \tan \phi = A_{vf} f_y \mu \tag{2.2}$$

where μ is 1.7 for monolithic concrete, 1.4 for intentionally roughened surface, and 0.8 to 1.0 for ordinary shear planes with contacting steel interfaces. The frictional force, μP, resists the sliding of the elements. To provide sufficient safety warnings in advance, shear connector systems are designed for a ductile failure rather than a brittle failure. To this effect, the reinforcement ratio is limited to a maximum of 0.015 such that the shear connectors will yield and fail before the concrete elements fail. In addition, it is also recommended that the shearing stress should not exceed 0.8 ksi (5.5 MPa) for concrete with a compressive strength of 4 ksi (28 MPa) or higher.

The Mohr-Coulomb equation can be used to estimate the shear stress, v, and is commonly used in soil and rock systems. Figure 2-2(a) shows a schematic of two elements in shear and the stress and displacement variables. Figure 2-2(b) shows the variation of stress as a function of shear displacement, δ_s. It also shows the Mohr-Coulomb equations for peak and sustained stresses. Note that c is the cohesive strength of the material in the shear plane, σ_n is the normal stress, ϕ is the angle of internal friction, and, ϕ_{sus} is the sustained angle of internal friction.

Graphical representations of these Mohr-Coulomb equations are provided in Figure 2-2(c) and shows that the peak and sustained stresses vary linearly as a function of normal stress.

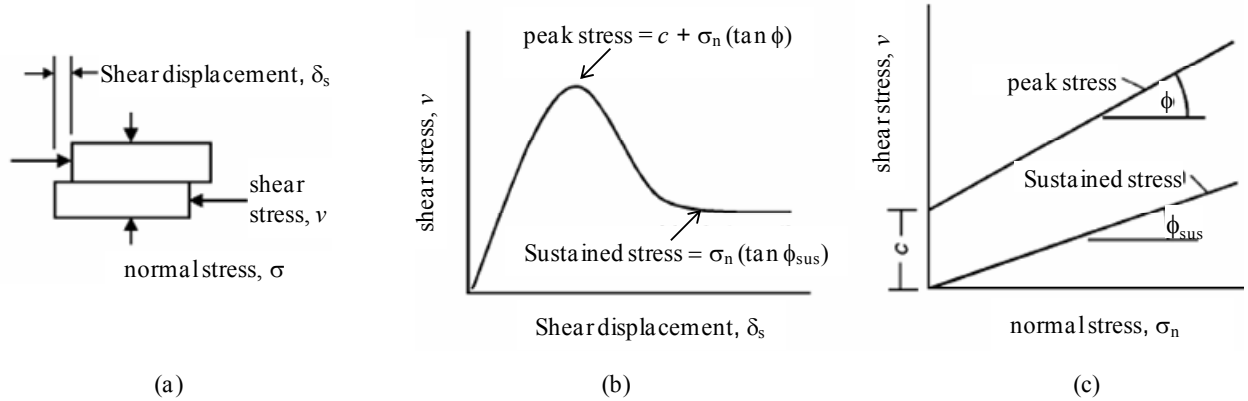

Figure 2-2. Shear stress behavior using Mohr-Coulomb Equation (Coulomb 1776)

The equation in the American Association of State Highway and Transportation Officials – Load and Resistance Factor Design – Bridge Design Specifications (AASHTO LRFD 2007) is analogous to the Mohr-Coulomb equations. In AASHTO LRFD (2007), the nominal peak shear stress, $v_{peak,\,n}$, is expressed as follows:

$$v_{peak,\,n} = c + \sigma_n \tan\phi \tag{2.3}$$

where the c, σ_n, and, ϕ are as defined in Figure 2-2. For practical applications, the term c depends on the surface roughness and is equal to the shear stress at zero normal stress. After sufficient slip or shear displacement occurs, the term c becomes zero and the sustained shear stress, v_{sus}, is expressed as follows [AASHTO LRFD (2007)]:

$$v_{sus} = \sigma_n \tan\phi_{sus} \tag{2.4}$$

where σ_n and ϕ_{sus} are as defined in Figure 2-2. For roughened surfaces as shown in Figure 2-3, the shear stress can be expressed as follows (Patton 1966):

$$v_r = \sigma_n \tan(\phi_b + i) \tag{2.5}$$

where ϕ_b is the basic friction angle of the surface, and i is the angle of the sawtooth. It is believed that as the shear displacement increases, the sawtooth surface behaves as a physical interlock on the shear planes. When the sawtooth is intact, the normal displacement leads to an increase in the normal stress on the shear connector. This is similar to the hypothesis of Birkeland and Birkeland (1966). However, the equation developed by Patton (1966) has an additional term (i.e., ϕ_b of the surface) to consider the initial friction condition.

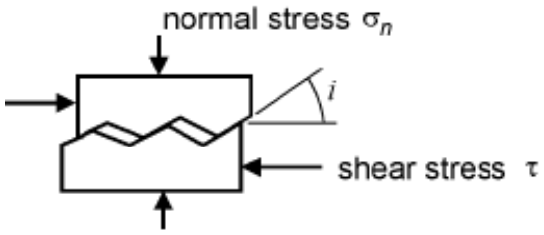

Figure 2-3. Roughened shear friction hypothesis (Patton 1966)

Recently, Mattock (2001) concluded that the shear friction is resisted by two major components: the undulations on the roughened surfaces, and the frictional stress provided by the clamping force resulting from the normal displacement caused by the separation of the roughened surfaces. This is reasonable because the main principle of shear friction theory was developed based on the behavior of under-reinforced shear plane.

2.3. STEEL GIRDER AND CONCRETE COMPOSITE SYSTEM

Rezansoff and Hosain (1983) investigated the shear behavior of a stud-girder connection in a steel girder-CIP deck system to evaluate the required number of shear studs. The effect of the

orientation of the applied load was also studied. The researchers recommended a small number of shear connectors to induce ductile failure of the shear stud and allow slip. The expected mechanism is analogous to the ductile failure of an under-reinforced beam, where flexural reinforcement yields and fails before the concrete fails.

2.4. CODE DEVELOPMENT

2.4.1. The American Association of State Highway and Transportation Officials Design

Article 5.8.4 in AASHTO LRFD (2007) requires a standard design concept and calculation formula for shear connections on precast girder and deck systems as follows:

$$\phi \cdot V_{ni} \geq V_{ui} \tag{2.6}$$

where V_{ni} is the nominal interface shear resistance (kips [N]), V_{ui} is the factored interface shear force due to the applied load, and ϕ is the reduction factor for the shear resistance.

When a CIP concrete slab is placed on a clean concrete girder surface roughened to an amplitude of 0.25 in. (6.4 mm), the nominal interface shear resistance is taken as follows [AASHTO LRFD (2007)]:

$$V_n = \underbrace{c \cdot A_{cv}}_{\substack{\text{concrete} \\ \text{contribution}}} + \underbrace{\mu \cdot (A_{vf} \cdot f_y + P_c)}_{\substack{\text{contributions from} \\ \text{steel connector and normal load}}} \tag{2.7}$$

$$V_{ni} \leq \begin{cases} K_1 f_c' A_{cv} \\ or \\ K_2 A_{cv} \end{cases} \tag{2.8}$$

where c = cohesion factor (0.28 ksi [1.9 MPa]); A_{cv} = interface area of the concrete engaged in shear transfer (in.^{2} [mm^2]); μ = coefficient of friction (1.0 for roughened concrete surface to an amplitude of 0.25 in. (6.4 mm)); A_{vf} = cross section of the shear reinforcement (in.^{2} [mm^2]); f_y = yield strength of the shear reinforcement (ksi [MPa]); P_c = net compressive force normal to the shear plane (kips) (conservative if P_c is neglected); K_1 = fraction of concrete strength available to resist the interface shear (0.3); and K_2 = limiting interface shear resistance and can be taken as 1.8 ksi [12.4 MPa] for normal-weight concrete or 1.3 ksi [8.9 MPa] for lightweight concrete. The upper limits should be defined to prevent brittle failure of the concrete (that can occur if the shear plane is over-reinforced) before the yielding of the steel (Birkeland and Birkeland 1966; and Mattock 2001). Note that c is cohesive force in the previous discussions in this report. However, in AASHTO LRFD (2007), it is defined as the cohesion factor and is used to capture the effects of cohesion and/or aggregate interlock. As shown in Eq. (2.7), the horizontal shear resistance consists of contributions from the concrete surface, the steel connectors, and the normal load. Note that Eqs. (2.7) and (2.8) are for applications when R-bars are used and if the amplitude of the roughened surface is less than the 0.25 in. (6.4 mm) specified, AASHTO LRFD (2007) requires that the coefficient of friction, μ, be reduced to 0.6.

2.4.2. American Concrete Institute (ACI) Design

The ACI 318-08 (2008) code provides the following expression for shear resistance:

$$V_n = \mu \cdot f_y \cdot A_{vf} \tag{2.9}$$

where V_n is the nominal shear strength; μ is the coefficient of friction; f_y is the yield strength of the shear connector (ksi [MPa]); and A_{vf} is the area of the shear transfer reinforcement (in.^{2} [mm^2]). This equation is valid when the shear connector is perpendicular to the shear plane. The recommended value of μ is 1.4 for normal-weight concrete placed monolithically. The recommended value of μ is 1.0 for normal-weight concrete placed against another concrete surface roughened to 0.25-in. (6.4 mm) amplitude. For normal-weight concrete anchored to as-rolled structural steel beams with headed studs or reinforcing bar connectors, the

recommended value of μ is 0.7. For these cases, when lightweight concrete is used, the recommended value of μ is further reduced by 25 percent (i.e., 0.5). Eq. (2.9) is generally used to estimate the quantity of shear connectors. To achieve a ductile failure of the systems with normal-weight concrete, either placed monolithically or placed against an existing hardened concrete with intentionally roughened surface, ACI 318-08 (2008) provides the following upper limits for the Eq. (2.9):

$$V_n \le \begin{cases} 0.2 f_c A_{cv} \\ (480 + 0.08) f_c A_{cv} \\ 1600 A_{cv} \end{cases} \tag{2.10}$$

where A_{cv} is the interface area of the concrete engaged in shear transfer (in.^{2} [mm^2]). For other cases, ACI 318-08 (2008) provides the following upper limits for the Eq. (2.9):

$$V_n \le \begin{cases} 0.2 f_c A_{cv} \\ 800 A_{cv} \end{cases} \tag{2.11}$$

If the above discussed ACI design equations are used, the value of the nominal shear strength, V_n, increases as the yield strength of reinforcement increases. However, Mattock and Hawkins (1972) and Mattock (2001) concluded that the rate of increase gradually decreases to a constant value of approximately 0.8 instead of the constant value of μ, which is 1.4 for normal-weight concrete (per ACI 318-08 2008). Therefore, the following equation was proposed by ACI 318-08 Commentary, which was based on PCI Design Handbook (2004), Mattock et al. (1976), and Mattock (1974), for a better estimate of the nominal shear strength:

$$V_n = 0.8 f_y A_{vf} + A_c K_1 \tag{2.12}$$

where A_c is the area of concrete section for resisting the shear force (in.^{2}) and K_1 is 400 psi (2.76 MPa) for normal-weight concrete and 200 psi (1.38 MPa) for all-lightweight concrete. The

first term represents the traditional concepts of friction resulting from a clamping force. The second term represents the resistance from the shearing protrusions (causing roughness) on the shear plane and the dowel action of the reinforcement (ACI 318-08). According to Mattock et al. (1976), the slip distance corresponding to the maximum peak shear force was less than 0.05 in. (1.3 mm).

2.5. RESEARCH ON FULL-DEPTH PRECAST GIRDER SYSTEM

Scholz et al. (2007), Kovach and Naito (2008), the National Cooperative Highway Research Program (NCHRP 2008), and Trejo et al. (2009) conducted push-off tests and full-scale testing to improve the design of shear connectors for a girder-haunch-deck system. Sullivan (2007) made full-depth, large-scale, precast bridge deck panels and performed various tests. These tests included typical push-off tests to investigate the shear resistance performance. The performance of Grade 60 reinforcing bars and headed–studs (with a yield strength of 49 ksi [338 kPa]) as shear connectors were evaluated using push-off tests. Bars and studs with different diameters and various quantities were evaluated. The studs exhibited good ductility, but due to the relatively low tensile strength, a large number of studs were required in the shear pockets. When reinforcing bars (i.e., R-bars) were used as shear connectors, the intentionally roughened surface on the bottom side of precast deck panels did not assist in achieving higher shear resistance values. When the headed-studs were used as shear connectors, the interfacial failure occurred between the haunch and the beam and, therefore, the intentionally roughened surface was not governing the failure. Scholz et al. (2007) concluded that the shear resistance is the combination of the chemical cohesion and Coulomb friction caused by the clamping force. The researchers concluded that if the cohesive bond was broken (i.e., cracks form) at the shear plane then only the shear connector provided the shear resistance. Scholz et al. (2007) also reported that the initial peak load is the resistance offered by the cohesive bond (i.e., cA_{cv}), and a secondary, post-peak load is the shear resistance offered by the shear connectors ($\mu(A_s f_y + P_n)$). With this, the authors recommended the following equation for designing shear connectors:

$$v_n = \max \begin{cases} cA_{cv} \\ \mu(A_s f_y + P_n) \end{cases} \tag{2.13}$$

where:

- c is the cohesive force (assumed to be equal to 0.075 ksi [0.52 MPa]),
- A_{cv} is the interface shear area;
- μ is the frictional coefficient (0.9 for a grout on concrete-concrete interface, 0.6 for a grout-steel interface),
- A_s is the cross-sectional area of the shear connector,
- f_y is the yield stress of the shear connector, and
- P_n is the additional normal force from external loads.

Kovach and Naito (2008) investigated the shear friction of girder-deck systems without shear connectors. They reported that the cohesion and adhesion between the girder and deck could provide sufficient shear resistance. In addition, the authors concluded that the interface roughness had a pronounced effect on the composite shear action and a sufficient level of roughness could help obtain a high level of horizontal shear capacity. Therefore, the surface condition, cohesion, and adhesion should be considered for the design and practice.

NCHRP (2008) investigated the shear capacity of headed-studs as shear connectors between concrete panels and structural steel girders. The researchers conducted push-off tests on the systems with four and eight headed-studs (each 1.25-in. [32 mm] in diameter). To improve the interface shear capacity, cross ties and steel tube systems were used to confine the grout in the shear pocket that surrounds the shear connectors. The testing indicated that push-off tests are sufficient to reflect the performance of full-size specimens. They found that the HSS (hollow structural section) steel tubes could effectively confine the grout that surrounds the shear studs in the shear pockets. However, test results showed high peak loads with relatively low ductility. Based on this study, design recommendations to achieve the peak shear resistance of the system were proposed.

The reports from the previous phases of TxDOT project 0-6100 evaluated shear connector capacities of different connector systems for full-depth precast panel systems (Trejo et al. 2009). The performance of the grout material in the haunch and other parameters that can affect the shear capacity of the system was evaluated. It was noted that the roughness of the

interfaces between the deck, haunch, and girder are more dependent on the secondary and post-peak shear strength than the initial peak shear strength. Note that the initial peak strength is a function of the cohesion only. Preliminary results from unroughened specimens indicated a friction factor of approximately 0.4. The testing with roughened concrete surfaces indicated a friction factor of 0.6 to 0.8. As a result of this low friction factor, many shear pockets and shear connectors were required to match the capacity of the R-bar system used in the current TxDOT design. In addition, when thicker haunches (say 3.5 in. [89 mm]) were assessed, sufficient shear capacity and ductility could not be achieved. The report recommended a system with a large number of shear pockets for a bridge overhang system. However, requiring a large number of shear pockets could pose many constructability and economical issues. Therefore, further research was recommended to evaluate different systems with reduced number of shear pockets leading to a more constructible and economical design.

3. EXPERIMENTAL PROGRAM

3.1. INTRODUCTION

This section presents the experimental program adopted for this research. A simplified schematic of the push-off test sample and experimental design is presented first. The characteristics of the materials used in the test program are then presented. The detailed design and layout of different series of push-off test specimens are then presented. Following this, the push-off test procedures are presented. Note that the experimental design was developed with close collaborations with TxDOT personnel. A full factorial test design and full-scale tests were not possible due to time and cost constraints.

3.2. PUSH-OFF TEST SAMPLE AND EXPERIMENTAL DESIGN

Push-off test samples were designed to assess the performance of different shear connector designs. Figure 3-1 shows a simplified schematic of a push-off sample tested in the laboratory. A shear pocket system consists of shear connectors and couplers, filling materials in a shear pocket, and any confinement system (i.e., reinforcement hoops or HSS [hollow structural section] steel tube).

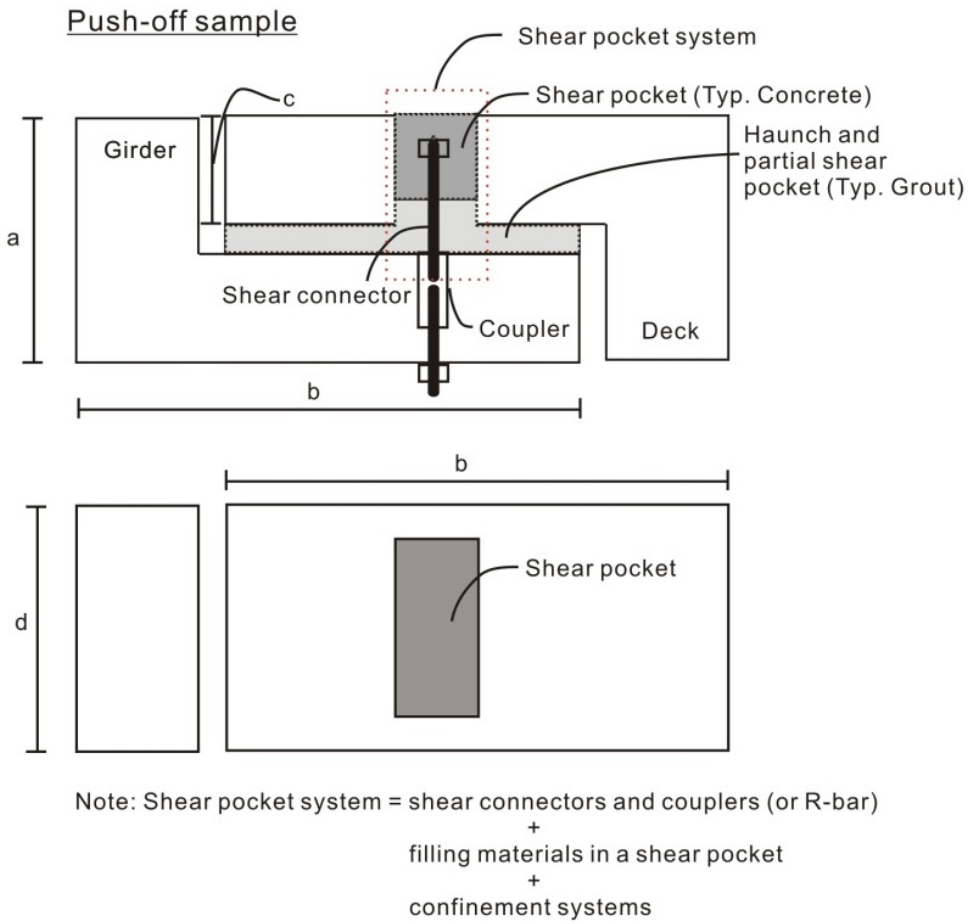

Figure 3-1. Simplified schematic of a push-off sample showing the elements representing the girder, deck, haunch, and shear connectors

Each push-off test sample consists of the following four major elements:

- a girder with embedded shear connector couplers (referred to herein as the girder element),
- a precast deck panel containing a single shear pocket (referred to herein as the deck element),
- a haunch between the girder and deck, and
- a shear connector system.

Figure 3-2 shows the naming convention used to identify the series of shear connector samples. For example, S2-0.62-IO represents a series containing two [2] shear connectors and couplers [S] within total cross-sectional area, A_{sc}, of 0.62 in.^{2} (400 mm^2) [0.62], with

confinement at both the inside [I] and outside [O] of the shear pocket. Shear connector couplers were embedded in the girder element such that the all-thread rods (i.e., shear connectors) can be post-installed to connect the girder element to the deck element.

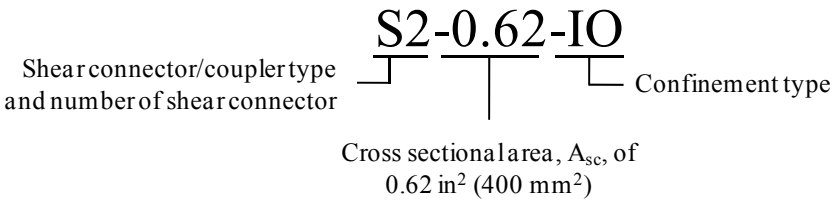

Figure 3-2. Naming convention for the shear connector series

Two types of shear connector/couple systems (R: R-bar and S: shear connector/coupler system) were tested. The effects of the following five confinement conditions were evaluated.

- N: No confinement;
- I: Inside the shear pocket;
- O: Outside the shear pocket;
- IO: Both inside and outside the shear pocket; and
- O[H]: HSS steel tube outside the shear pocket.

The following eight series of push-off samples were designed and fabricated: R2-0.4-N, S2-0.62-N, S2-0.62-I, S2-0.62-O, S2-0.62-IO, S2-1.83-N, S2-1.83-IO, S4-3.66-O[H]. Three replicate samples of each of these series were fabricated and tested for shear capacity.

3.3. MATERIALS

This section presents characteristics of the materials used for the push-off test program.

3.3.1. Concrete

Ready-mix concrete from a local plant was procured for preparing the girder and deck elements of the push-off test specimens. This concrete is denoted as 'push-off concrete,' herein. The

push-off test specimens were cast in the High Bay Structural and Materials Laboratory (HBSML) at Texas A&M University, College Station, Texas. The concrete placed in the shear pockets was prepared in the HBSML laboratory and is denoted as 'shear pocket concrete,' herein. The mixture proportion was such that the shear pocket concrete will have similar characteristics as that of the push-off concrete. The mixture proportions of both these concrete mixtures are shown in Table 3-1.

Table 3-1. Mixture proportions for concrete mixtures

Properties	Ready-mix concrete used to make Push-off Samples	Lab-mixed concrete placed in Shear Pockets
Type I Cement, lb/yd^3 (kg/m^3)	508 (302)	508 (302)
Fly ash, lb/yd^3 (kg/m^3)	197 (117)	197 (117)
Coarse agg., lb/yd^3(kg/m^3)	1783 (1058)	1816 (1077)
Fine agg., lb/yd^3 (kg/m^3)	1110 (659)	1160 (688)
Admixtures, oz/yd^3 (L/m^3)	Unidentified	68 (2.63)
Water-to-cement ratio, w/c	0.43	0.43

The compressive strengths of 4×8 in. (102×203 mm) cylinders at the time of the push-off tests were determined in accordance with ASTM C39, *Standard Test Method for Compressive Strength of Cylindrical Concrete Specimens* (2007), and the results from these tests are provided in the second and third columns of Table 3-2. For girder and deck elements, TxDOT Class S concrete was used and it is normally proportioned for a minimum compressive strength of 4 ksi (28 MPa). The push-off concrete samples exhibited compressive strengths ranging from 5.9 to 7.5 ksi (41 to 52 MPa). The shear pocket concrete had the compressive strengths ranging from 7.3 ksi to 10 ksi (50 to 69 MPa).

Table 3-2. Compressive strength of concrete and grout at the time of push-off test

Series Name of the Push-off Samples	Push-off Sample Concrete, ksi (MPa)	Shear Pocket Concrete, ksi (MPa)	Haunch Grout, ksi (MPa)
R2-0.4-N	6.6 (45)	Data not available	7.4 (51)
S2-0.62-N	7.5 (52)	8.2 (56)	6.9 (47)
S2-0.62-I	7.6 (53)	9.6 (66)	6.3 (43)
S2-0.62-O	6.1 (42)	7.3 (51)	6.1 (42)
S2-0.62-IO	6.1 (42)	7.3 (51)	6.1 (42)
S2-1.83-N	5.9 (41)	7.9 (55)	6.3 (44)
S2-1.83-IO	6.6 (45)	10 (69)	8.1 (56)
S4-3.66-O[H]	6.6 (46)	7.9 (55)	7.5 (52)

3.3.2. Grout

In addition to the two types of concrete, two types of grout (i.e., BASF Set 45 and SikaGrout™ 212) were also used in this test program. The BASF Set 45 is magnesium phosphate-based and the SikaGrout™ 212 is a non-shrinking hydraulic cement structural grout meeting the ASTM C1170 *Standard Specification for Package d Dry, Hydraulic-Cement Grout* (2007). To measure the consistency and cohesiveness, the flow cone test was performed following the method used by Trejo et al. (2009). The diameter of the grout patty at the end of the flow cone test was a measure of the consistency and cohesiveness of the grout mixture. The target diameter was determined to be at least 8 in. (203 mm) such that the mixture is sufficiently consistent and cohesive. Based on preliminary trial mixtures, it was determined that a water-powder ratio (w/p) of 0.065 was suitable for the BASF Set 45 grout and a w/p of 0.14 was suitable for SikaGrout™ 212. The compressive strength of 2-in. (50 mm) grout cubes was determined in accordance with the ASTM C109, *Standard Test Method for Compressive Strength of Hydraulic Cement Mortars (Using 2-in or [50mm] Cube Specimens)* (2008), and the results from these tests are shown in the fourth column of Table 3-2. The compressive strengths of grout samples ranged from 6.1 to 8.1 ksi (42 to 56 MPa).

3.3.3. Reinforcement and Shear Connectors

Grade 60 reinforcement meeting the ASTM A615, *Standard Specification for Deformed and Plain Carbon-Steel Bars for Concrete Reinforcement* (2008), was used in the push-off samples. The 1.25- and 0.75-in. (32 and 19 mm) diameter all-thread rods (Product No. B-12 manufactured by Dayton Superior) were used as shear connectors, as recommended by TxDOT personnel. Table 3-3 shows the yield and tensile strength (or stress) and strains of the reinforcement and shear connectors used in this research. Closed couplers were used to connect the shear connectors (Product No. B-32 manufactured by Dayton Superior). For the 0.75-in. (19 mm) diameter all-thread rods, the length and the outer diameter of the coupler were 3.0 and 1.1 in. (76 and 27 mm), respectively. For the 1.25-in. (32 mm) diameter all-thread rods, the length and the outer diameter of the coupler were 5.5 and 1.9 in. (140 and 48 mm), respectively. In this study, there was no failure associated with the couplers. This indicates that the coupler provided sufficient capacity for the shear connector.

Table 3-3. Mechanical properties of reinforcement and shear connectors

Sample I.D.	Yield strength, f_y, ksi (MPa)	Yield Strain, ε_y, x10^{-6} in./in. (mm/mm)	Ultimate Strength, f_u, ksi (MPa)	Ultimate Strain, ε_u, × 10^{-6} in./in. (mm/mm)	Modulus of Elasticity, E, ksi (GPa)
#4 (M 13) reinforcement	62 (428)	2200	97 (669)	-	29,000 (200)
0.75-in. (19 mm) diameter shear connector	110* (759)	5800	123 (848)	22,400	28,060 (193)
1.25-in. (32 mm) diameter shear connector	97* (669)	5260	116 (800)	28,300	29,600 (204)

Note: * yield strength and strain are determined from 0.2 percent offset strain.
"-" indicates that data is not available.

3.4. Fabrication of Push-Off Test Samples

All the push-off test specimens were fabricated in the High Bay Structural and Materials Laboratory at Texas A&M University, College Station, Texas. Following is a brief discussion

on the reinforcement layout, the shear connector layout, and the alignment of girder and deck elements, and the process of filling the haunch and shear pockets.

3.4.1. Reinforcement Layout

For the samples in the R2-0.4-N series, the layout of reinforcement was similar to that in the samples used in the research by Scholz et al. (2007). The samples in S2 and S4 series contain #5 (M16) and #4 (M13) reinforcement, respectively, to mimic the detail of a typical girder-haunch-deck system in a bridge. The samples in S4-3.66-O[H] series resembled the deck panel used in the NCHRP (2008) study, except for the detail of shear connector system and shear pocket design.

3.4.2. Shear Connector Layout and Shear Pocket Confinement

Trejo et al. (2009) found that lack of confinement of the portion of the shear connector/coupler inside the girder resulted in premature failure of the anchorage of the shear connector/coupler. Therefore, two bundled hoops [#4 (M13)] were placed to confine the concrete surrounding the shear couplers to prevent the premature failure of the anchorage of the shear connector/coupler systems in the push-off test specimens. Similar hoops were also provided in the shear pockets to confine the concrete/grout around the all-thread rods in the deck elements. Table 3-4 shows the type, number, and diameter of shear connectors and the type of confinement in the shear pockets. It should also be noted that this test assumes that the concrete around the couplers embedded inside the girder is well-confined, and will not fail. Note that the design for the S series shear connectors was determined using an increased haunch depth. Also, rectangular pockets were preferred for the design of precast deck and the placement of multiple shear connectors.

Table 3-4. Detailed shear connectors and shear pockets

Series Identification	Connection Type	Number of Shear Connectors and its Diameter	A_{sc} in^2 (mm^2)	Interface shear plan area, In.^{2} (m^2)	Confinement Condition of the Concrete around the Shear Connector in the deck	Normal Force kips (kN)
R2-0.4-N	R-bar	2 legs (0.50-in.)	0.40 (258)	416 (0.26)	None [N]	2.5 (11)
S2-0.62-N	Shear Connector /Coupler	2 (0.75-in.)	0.62 (400)	416 (0.26)	None [N]	1.3 (5.8)
S2-0.62-I		2 (0.75-in.)	0.62 (400)	416 (0.26)	Inside [I]	1.3 (5.8)
S2-0.62-O		2 (0.75-in.)	0.62 (400)	416 (0.26)	Outside [O]	1.3 (5.8)
S2-0.62-IO		2 (0.75-in.)	0.62 (400)	416 (0.26)	Both inside and outside [IO]	1.3 (5.8)
S2-1.83-N		2 (1.25-in.)	1.83 (1180)	416 (0.26)	None [N]	1.3 (5.8)
S2-1.83-IO		2 (1.25-in.)	1.83 (1180)	416 (0.26)	Both inside and outside [IO]	1.3 (5.8)
S4-3.66-O[H]		4 (1.25-in.)	3.66 (2361)	696 (0.45)	Outside the shear pocket with HSS tube, O[H]	1.3 (5.8)

3.4.2.1. R2-0.4-N Series Push-off Samples

R-bars are widely used in girders for CIP deck systems on bridges. Figure 3-3 shows the schematic of the R2-0.4-N series push-off sample using conventional R-bars as the shear connectors. The #4 (M13) R-bars were embedded into the girder when the girder was cast. The deck element has a 6 in. (152 mm) diameter shear pocket through the entire depth of the deck. When assembling the girder elements and deck elements, the 2-in. (50 mm) thick haunch and the shear pocket were filled with the BASF Set 45 grout.

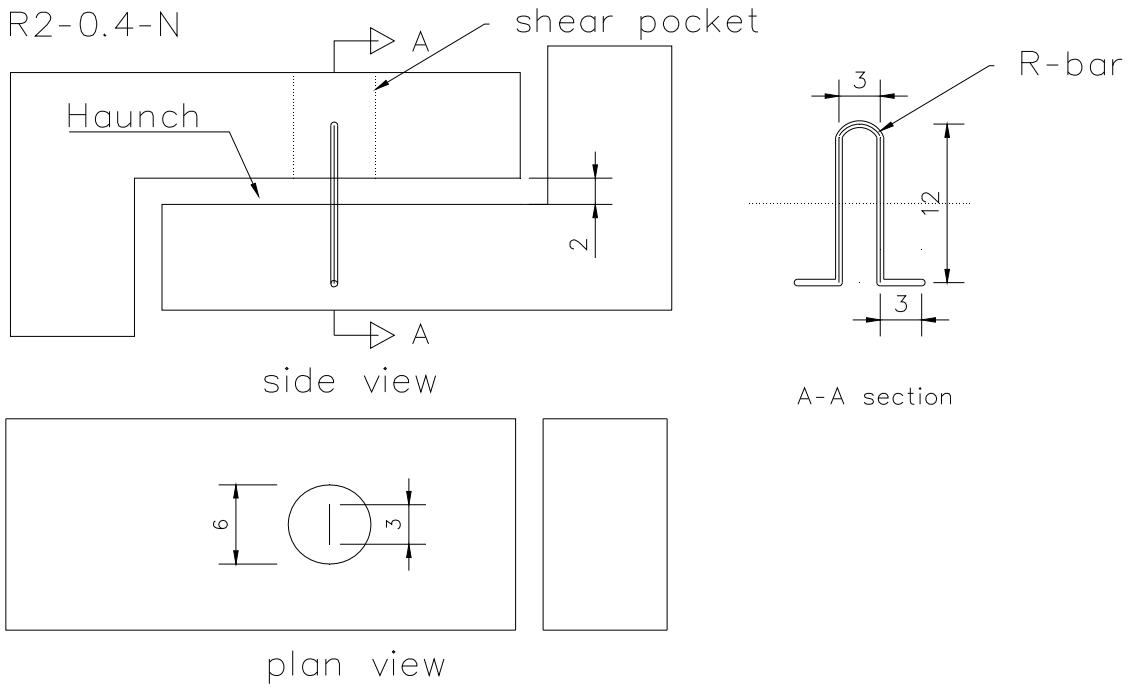

Figure 3-3. Schematic of R2-0.4-N series push-off samples with R-bar systems

3.4.2.2. S2-0.62 Series Push-off Samples

As shown in Table 3-4, the push-off samples in the S2 series had two shear connectors embedded into the deck panel. In addition, four types of confinement (i.e., N, I, O, and IO) around the two shear connectors (0.75-in. [19 mm] diameter) were tested. In the S2-0.62-N series push-off samples, the deck element had a 5×10 in. (127×254 mm) shear pocket with no reinforcement for confinement (see Figure 3-4). The samples in the S2-0.62-I series had five layers of #3 (M10) hoops at 1.75 in. (45 mm) spacing. The distance from the centroid of reinforcement to the bottom surface of the girder is 1.5 in. (38 mm). These hoops were placed inside the shear pocket and surrounding the shear connectors (see Figure 3-5). The S2-0.62-O series push-off samples had three layers of #3 (M10) hoops at 1.75 in. (45 mm) spacing (see Figure 3-6). The distance from the centroid of reinforcement to the bottom surface of the deck is 1.5 in. (38 mm). These hoops were placed outside the shear pocket (see Figure 3-6). The S2-0.62-IO series push-off samples had hoops at both the inside and outside of the shear pocket in

the precast deck panel (see Figure 3-7). The hoops placed inside the shear pocket in the above samples were placed at the desired position before casting grout into the shear pocket (see Figure 3-7).

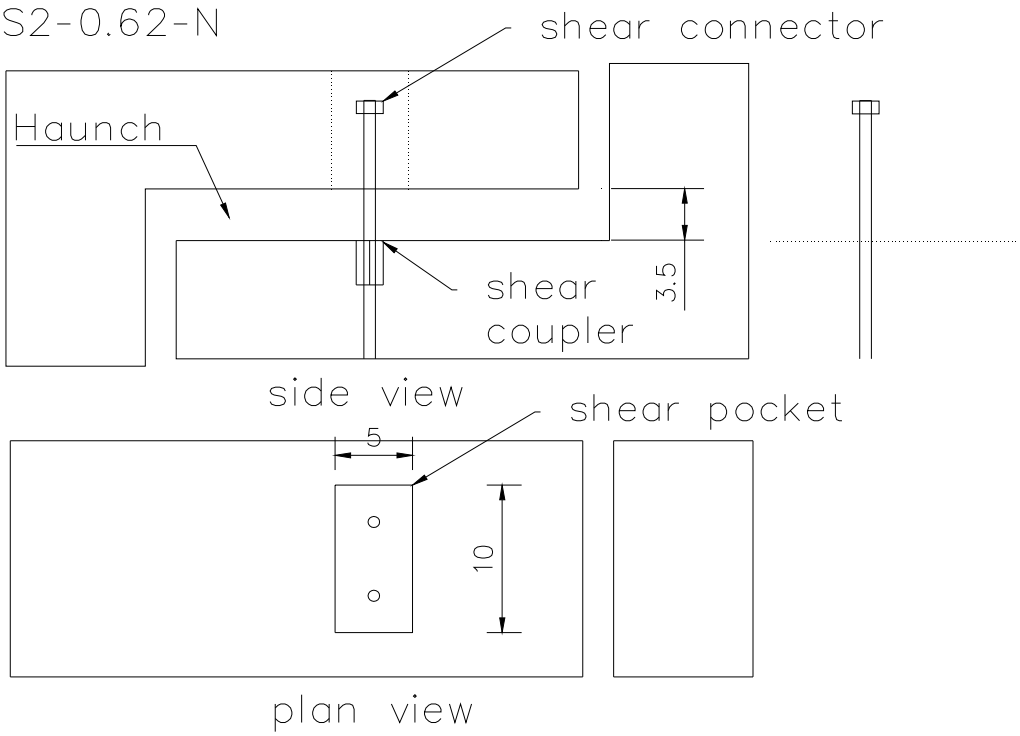

Figure 3-4. Schematic of S2-0.62-N series push-off sample (no confinement)

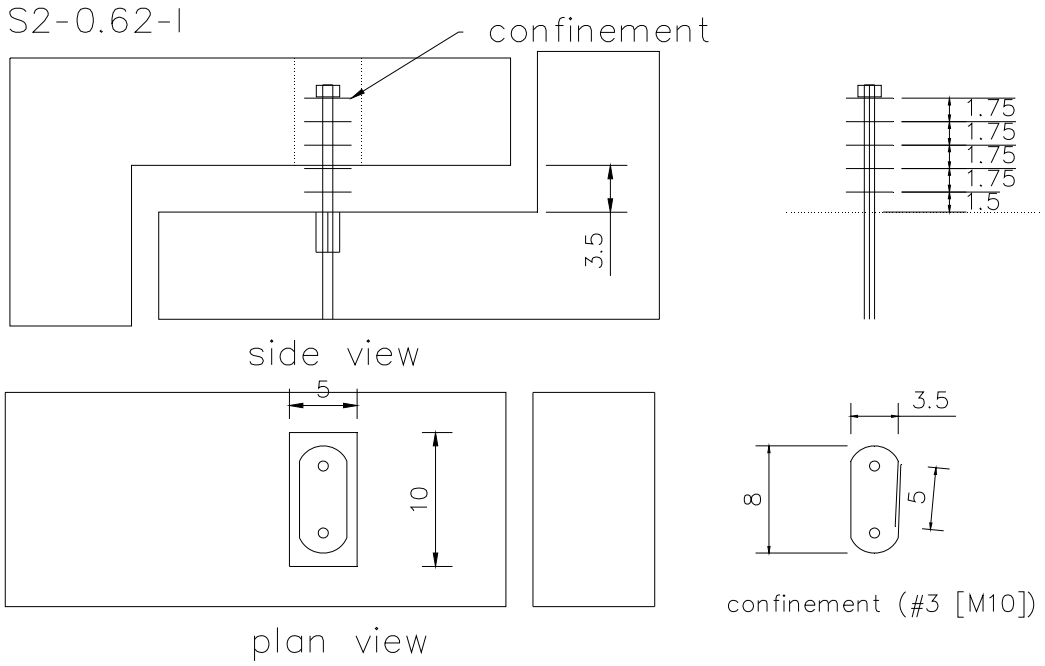

Figure 3-5. Schematic of S2-0.62-I series push-off sample (confinement is inside the shear pocket)

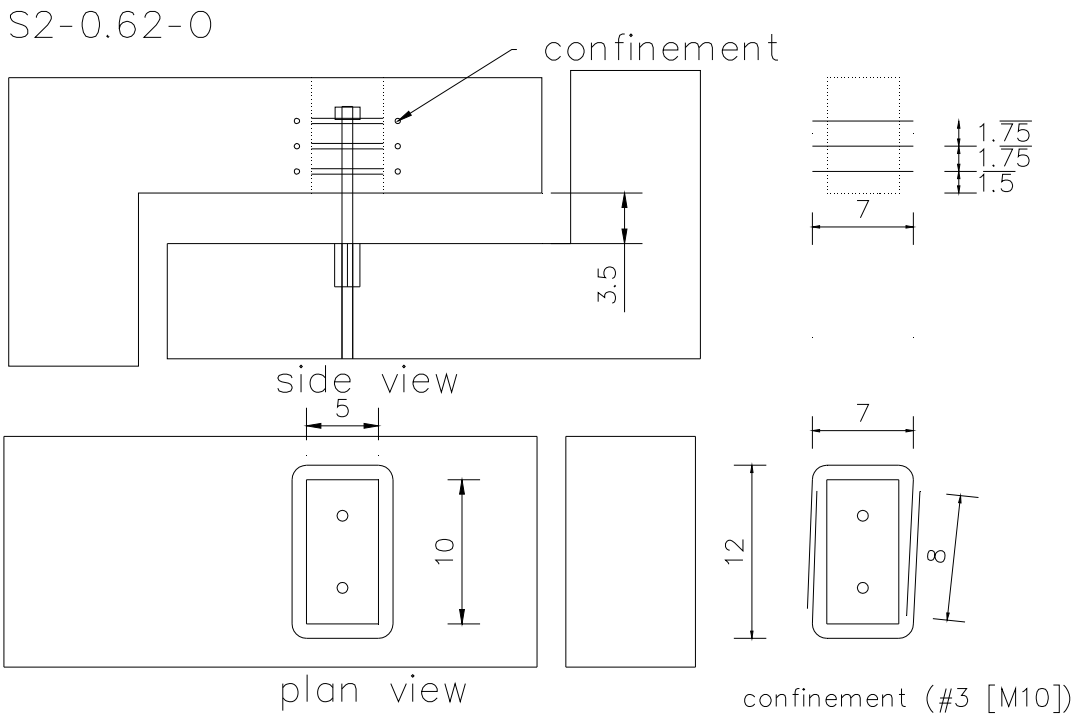

Figure 3-6. Schematic of S2-0.62-O series push-off sample (confinement is outside the shear pocket)

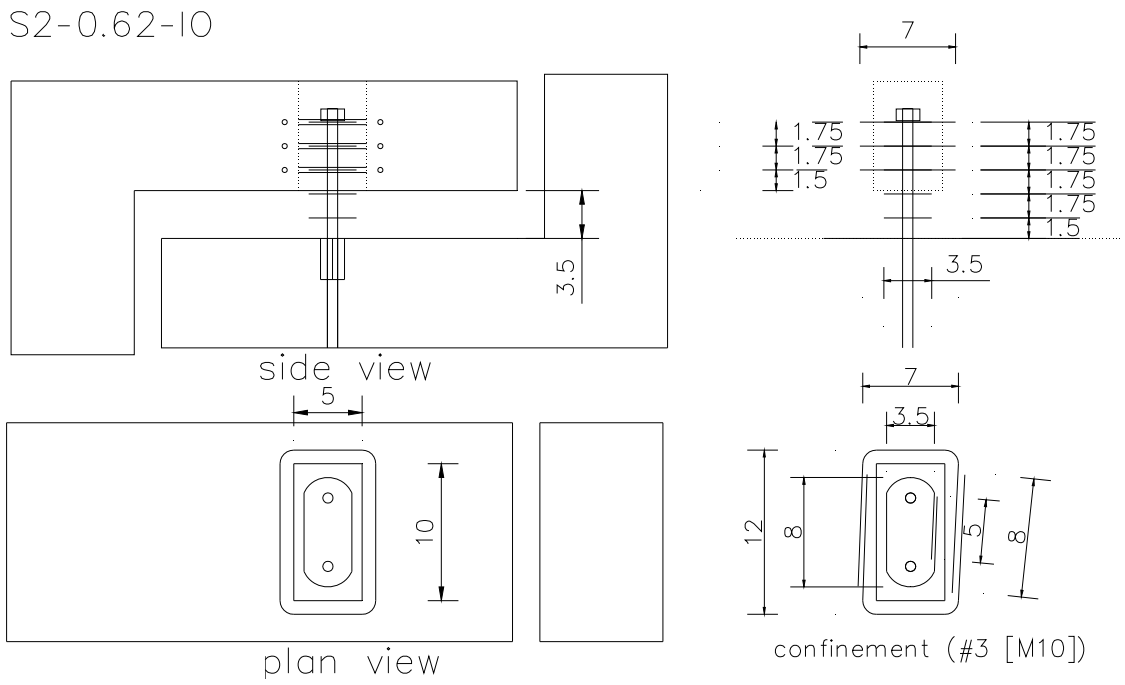

Figure 3-7. Schematic of S2-0.62-IO series push-off sample (confinement is at both the inside and outside of the shear pocket)

3.4.2.3. S2-1.83 Series Push-off Samples

As shown in Figure 3-8, the S2-1.83-N sample was designed to have two shear connectors (each 1.25 in. [32 mm] diameter) for the girder-haunch-deck system. The precast deck panel has an 8×10 in. (203 × 254 mm) shear pocket with no reinforcement for confinement. The shear connectors with nuts were post-installed into this shear pocket with 4 in. (102 mm) embedment length to resist shear force. As shown in Figure 3-9, the S2-1.83-IO series push-off samples were fabricated in a similar fashion as the S2-1.83-N series samples, except that hoops were provided at both the inside and outside of shear pocket (i.e., IO confinement). The 4 in. (102 mm) embedment length of the shear connectors into the deck resulted in three layers of hoops for the inside of shear pocket as compared to five layers for the S2-0.62-IO series containing 6 in. (152 mm) embedment length shear connectors. To confine the surroundings of shear connectors, three layers of outer shear confinement were placed with 1.5 in. (38 mm) spacing (see Figure 3-10).

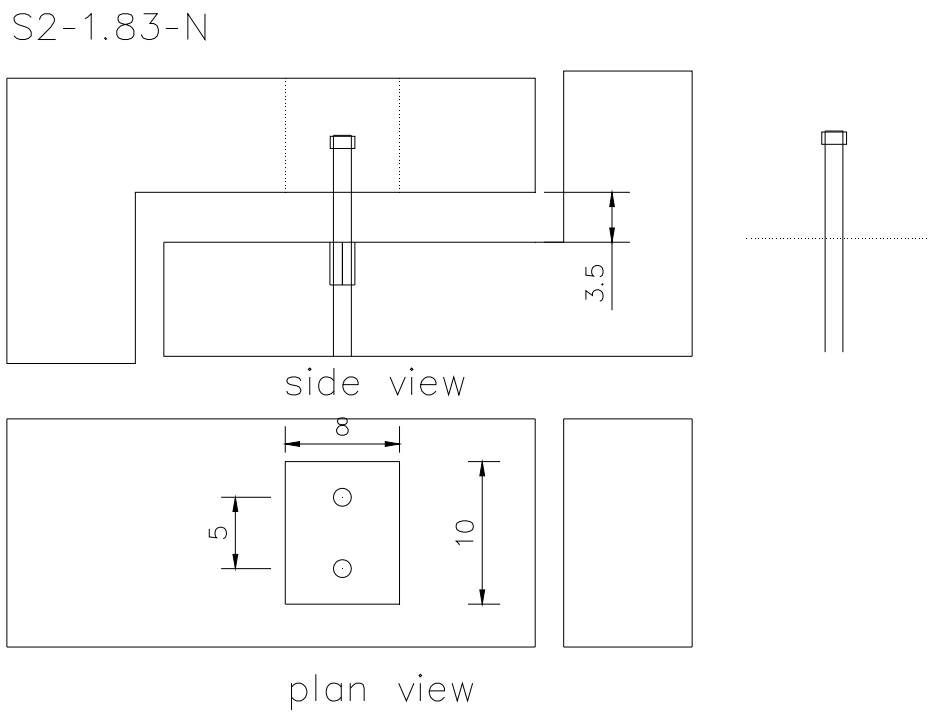

Figure 3-8. Schematic of S2-1.83-N series push-off sample (no confinement)

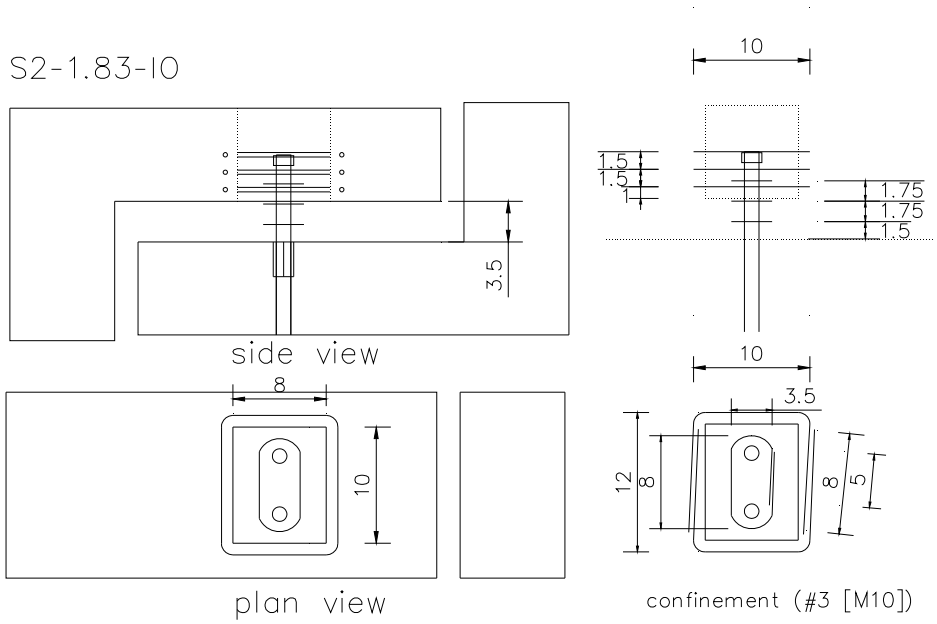

Figure 3-9. Schematic of S2-1.83-IO series push-off sample (confinement is at both the inside and outside of the shear pocket)

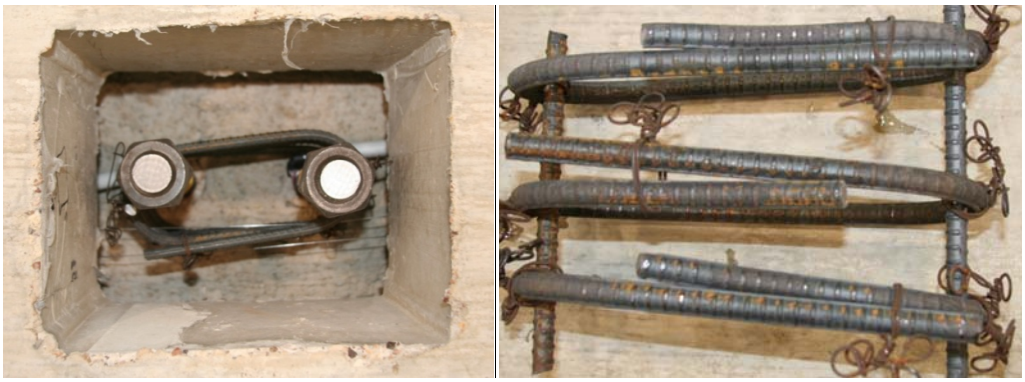

(a) (b)

Figure 3-10. Photographs: (a) Setup for proper positioning of the hoops inside the shear pocket; (b) an inner confinement

3.4.2.4. S4 Series Push-off Samples

As shown in Figure 3-11, the push-off samples in the S4-3.66-O[H] series had four 1.25-in. (32 mm) diameter shear connectors with 4 in. (102 mm) embedment lengths into the deck element. HSS structural steel tubes (6 in. [152 mm] long) were used to enclose the 8×10 in. (203×254 mm) shear pocket. The clear cover from the outer surface of the deck element to the top of embedded HSS structural steel tube was 2 in. (50 mm). As opposed to two shear connectors in the R2 and S2 series samples, S4 series samples had four shear connectors. The layout of these four shear connectors within a shear pocket is shown in Figure 3-11.

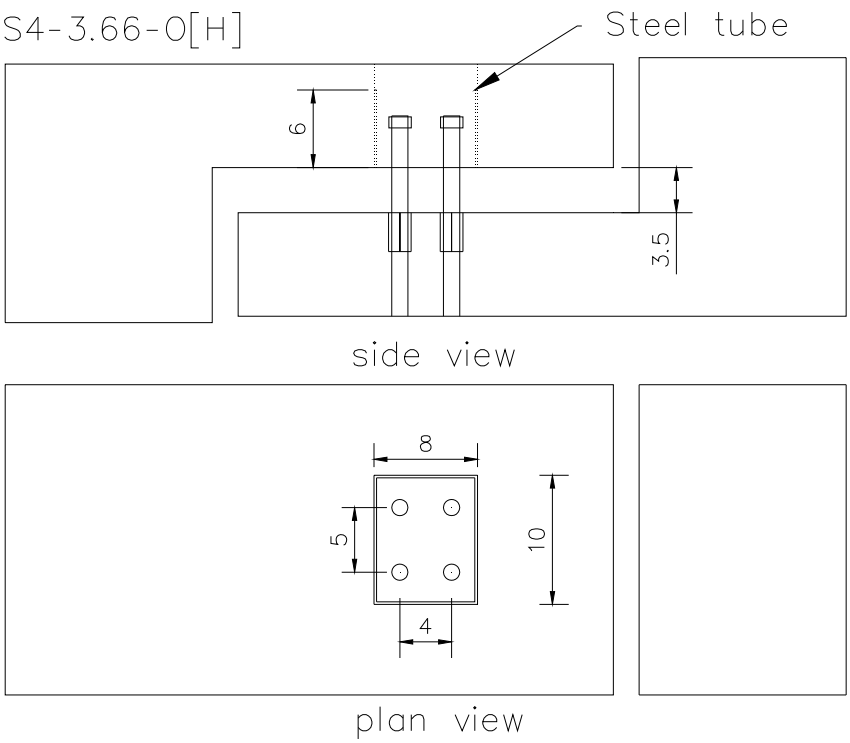

Figure 3-11. Schematic of S4-3.66-O[H] series push-off sample (HSS confinement outside the shear pocket)

3.4.3. Alignment of Deck and Girder Elements and Filling the Haunch and Shear Pockets of Push-off Samples

Trejo et al. (2009) developed appropriate forms to contain the fresh grout while filling the haunch. To ensure the desired haunch heights, forms and chairs of appropriate heights were placed in between the deck and girder elements. The haunch height was 2 in. (50 mm) for the R2-0.4-N series samples and was 3.5 in. (89 mm) for samples in all other series. Immediately after the initial setting, the concrete surface of the girder element was roughened using steel wire brushes. For all the samples, except the R2-0.4-N series samples, the haunch and shear pockets were filled with SikaGrout™ 212 grout up to 2 in. (50 mm) above the bottom of the deck panel (into the pocket). Then, after allowing the grout to set for approximately 15 to 30 minutes, the remaining space in the shear pockets was filled with shear pocket concrete. For the R2-0.4-N series samples, the haunch and shear pockets were completely filled with BASF Set 45 grout. In all the samples, the grout and/or concrete surfaces were finished and cured.

3.5. PUSH-OFF TEST PROCEDURES

3.5.1. Push-off Test Setup

A total of 24 push-off tests were conducted to investigate the shear transfer behavior of the girder-haunch-deck systems. Figure 3-12 shows the schematic of the push-off test setup.

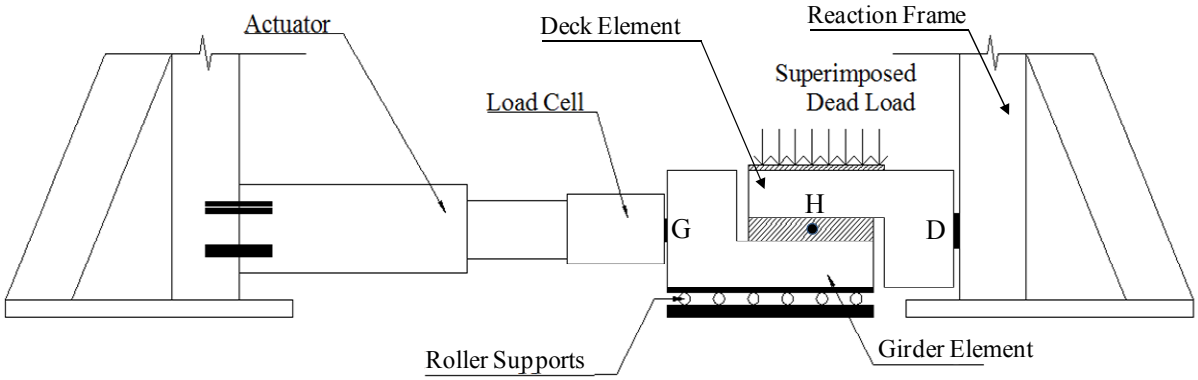

Figure 3-12. The push-off test setup

Six steel pipes (roller supports) were used to allow the girder element to slide without friction between the floor and the girder element. A 600-kip (270 ton) capacity actuator was used to apply the shear force to the deck element. A steel plate and a neoprene pad were inserted between loading apparatus and the deck element to prevent local crushing of the concrete. The elements of the push-off sample were positioned such that the midpoint G of the contact between the load cell and the girder element, the midpoint D of the contact between the reaction frame and the deck element, and the midpoint H of the haunch were on the same horizontal line. This provided a shear force on the girder-haunch-deck interface of the system with no bending or torsion. Based on the superimposed dead load used by Sullivan (2007), a 2.5-kip (11 kN) steel frame was placed on the deck to simulate the superimposed dead load for the testing of the samples in R2 series. However, while testing the samples in the S2 and S4 series, a 1.3-kip (6 kN) steel frame was placed on the deck element to simulate the typical tributary dead load on every pocket in an 8-ft long precast panel with five pockets. This value was used in the preliminary design of the Rock Creek Bridge in Parker County, Texas.

3.5.2. Instrumentation for Stress and Displacement Measurement

The strain gages were attached on the surface of the steel shear connectors. Four strain gages were installed such that the pure tensile stress on the shear connectors (i.e., excluding torsional and bending stresses) could be measured. Figure 3-13 shows the locations of the Linear Variable Differential Transformers (LVDT) and string potentiometers to measure the lateral and vertical displacements. Four LVDTs were installed in the horizontal direction to measure the horizontal slip (to compensate for the out-of-plane displacements [i.e., rotational displacement]) between the girder and the deck elements. In addition, four LVDTs and four string potentiometers were installed in the vertical direction to measure the vertical displacement between the girder and the deck elements (i.e., across the haunch thickness).

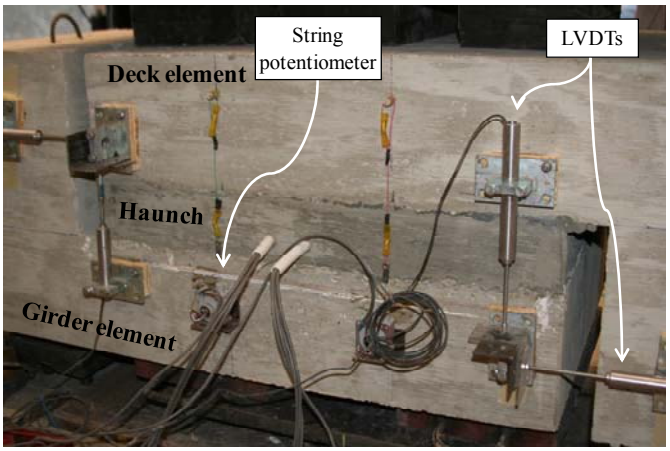

Figure 3-13. Instrumentations for displacement measurement

3.5.3. Rate of Loading during the Push-off Test

During the initial loading, a load control regime was adopted. Later, a displacement control regime was adopted. In the initial load control regime, the rate of loading was 7 kips/min. (31 kN/min.). After the load reached 30 kips (133 kN), further loading was applied with a displacement rate of 0.05 in./min. (1.3 mm/min.) until the load reached peak load. Due to the failure of cohesion or adhesion within the girder-haunch-deck systems, the load decreased during testing. After this drop in the load, the displacement rate was increased to 0.2 in./min. (5.0 mm/min.). Loading was stopped when the horizontal slip between the girder and deck elements reached 1.5 in. (38 mm).

4. TEST RESULTS AND ANALYSIS

4.1. GENERAL

Push-off tests were conducted to investigate various shear transfer and failure mechanisms in girder-haunch-deck systems. Five stages of shear transfer and failure mechanisms were identified during the testing:

- initial adhesion loss (Stage 1),
- shear key action (Stage 2),
- shear key action failure at peak load (Stage 3),
- dowel action of the shear connectors at sustained load (Stage 4), and
- final failure of the system (Stage 5).

In Stage 1, the adhesion between the components (i.e., girder, haunch, and precast deck) failed due to the shear load (defined as V_{loss} herein), resulting in the initial slip, which was less than 0.05 in. (1.3 mm). This, in turn, resulted in the stress concentration near a shear pocket system.

In Stage 2, the shear connectors and concrete and/or grout in the shear pocket acted as a shear key. The additional shear resistance was then provided by this shear key and the clamping force of the shear connectors.

In Stage 3, as the load increased, the shear key was sheared off or failed at the peak load (V_{peak}).

In Stage 4, after the shear key failed, the dowel action across the shear interface was the main source of shear resistance until the system failure occurred. This available shear resistance was defined as sustained shear resistance, V_{sus}. Figure 4-1 shows the mechanisms of shear key action and dowel action of the shear connectors. It should be noted that before the initiation of slip at the interface, there is no clamping force provided by the slab dead load. The clamping force occurs when the interface between the girder and deck are starting to separate as the shear

connectors build up stress. Figure 4-2 shows a typical plot of the interface shear load versus slip in the girder-haunch-deck systems. Stage 5 was failure of the system.

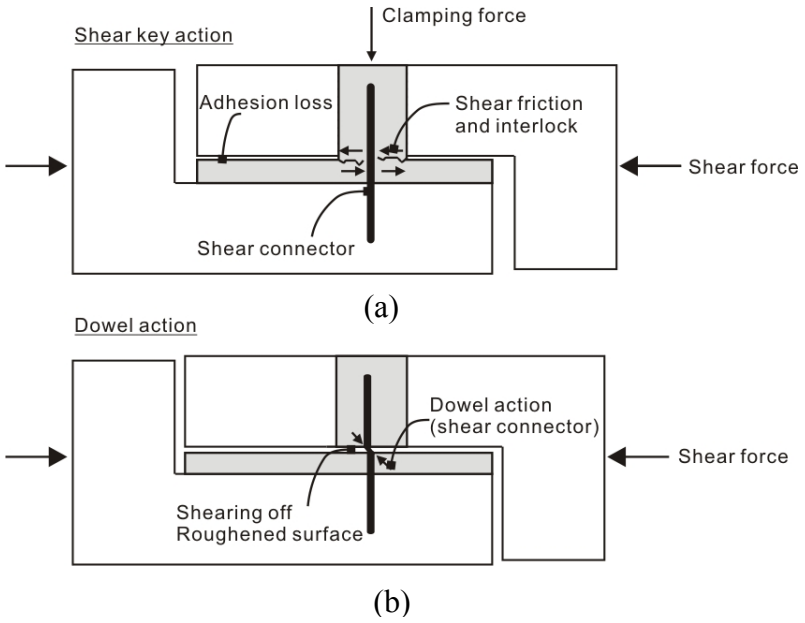

Figure 4-1. Mechanisms of shear connector systems: (a) Shear key action, (b) Dowel action

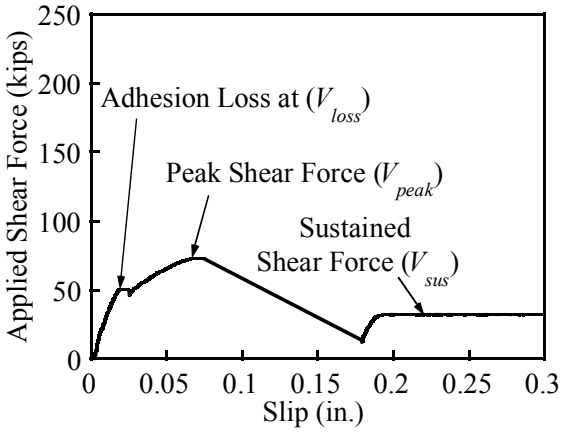

Figure 4-2. Typical failure mode and the plot of the system

Figure 4-3 shows three mechanisms of dowel action: a) the bending of the shear connector; b) the shearing of the shear connector; and c) the kinking of the shear connectors. To activate the dowel mechanisms, the anchorage zone in the girder and deck should be well-

confined by the surrounding concrete and/or grout. The modes of dowel action depend on the stiffness of shear connectors. According to Park and Paulay (1975), the failure of small diameter shear connectors tends to be governed by the kinking mechanism.

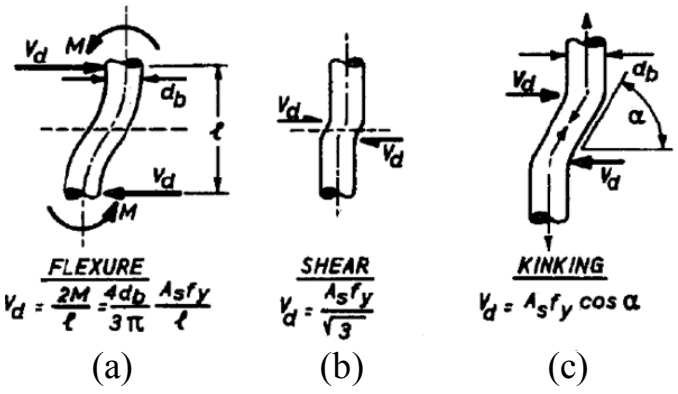

Figure 4-3. Three mechanisms of dowel action (Park and Paulay 1975)

The stiffness of the shear connectors and the bearing capacity of shear pocket concrete surrounding the shear connectors (i.e., concrete and/or grout capacity against the lateral shear force, V_d in Figure 4-3) influenced the sustained shear force and the final system failure. Four final system failure modes are as follows:

- anchorage failure,
- shear failure of the shear connector,
- tension failure of the shear connector (this is desirable failure mode), and
- interface failure between a pocket and a deck.

4.2. TEST RESULTS

Table 4-1 shows the applied shear loads at the loss of adhesion, at peak, and at 80 percent of peak sustained force along with the failure mode.

Table 4-1. Summary of test results

Series I.D.	Sample I.D.	V_{loss}, kips (kN)	V_{peak}, kips (kN)	0.8 V_{sus}, kips(kN)	Failure Mode
R2-0.4-N	1	-	55 (250)	33 (147)	BF
	2	52 (230)	75 (330)	35 (160)	BF
	3	50 (220)	73 (330)	34 (151)	BF
S2-0.62-N	1	63 (280)	83 (370)	66 (290)	BF
	2	54 (240)	79 (350)	60 (270)	BF
	3	50 (220)	76 (340)	60 (270)	BF
S2-0.62-I	1	54 (240)	81 (360)	54 (240)	BF
	2	54 (240)	78 (350)	56 (250)	BF
	3	55 (240)	97 (430)	76 (340)	BF
S2-0.62-O	1	48 (210)	87 (390)	54 (240)	BF
	2	45 (200)	66 (290)	45 (200)	BF
	3	62 (280)	89 (400)	56 (250)	BF
S2-0.62-IO	1	49 (220)	92 (400)	72 (320)	BF
	2	67 (300)	95 (420)	61 (270)	BF
	3	61 (270)	99 (440)	62 (280)	BF
S2-1.83-N	1	45 (200)	65 (290)	51 (230)	DDF
	2	42 (190)	68 (300)	54 (240)	DDF
	3	45 (200)	98 (440)	40 (180)	DF
S2-1.83-IO	1	61 (270)	99 (440)	-	DF
	2	58 (260)	113 (500)	-	DF
	3	-	118 (530)	-	DF
S4-3.66-O[H]	1	-	216 (960)	-	IF
	2	78 (350)	189 (840)	117 (520)	BF
	3	86 (380)	184 (820)	145 (650)	BF

Note: BF = bar failure; DF = deck concrete failure; DDF = ductile deck failure; IF=shear pocket adhesion loss; '-' indicates no data available.

4.3. FAILURE MECHANISMS IN R2 SERIES PUSH-OFF SAMPLES

The roughened surface of the girder element can provide strong adhesion between the girder and the haunch of a girder-haunch-deck system. However, the adhesion between the unroughened surface underneath the deck element and the haunch surface was typically weak. After adhesion loss, the shear pocket system resisted the shear force until the peak load. At the peak load, all the reinforcement (i.e., R-bars) began strain hardening. After the peak load, the dowel action (kinking) of the R-bars seemed to be the main source of resisting the shear load. It should be

noted that a girder-haunch-deck system does not perform in the same manner as a conventional girder-CIP deck system that does not have shear pockets. The shear key action provided by the shear pockets does not exist in the girder-CIP deck system in bridges. The girder-CIP deck system can exhibit higher adhesion between the roughened girder surface and the CIP deck. However, the post-peak behavior of the girder-haunch-deck system was similar to a CIP deck system after the adhesion failure of the interface between the deck concrete and girder.

Figure 4-4 shows the shear load versus slip for the R2-0.4-N samples containing a conventional R-bar. The average peak load and the 80 percent sustained load were 67 and 34 kips (300 and 150 kN), respectively. When the slip reached approximately 0.05 in. (1.3 mm), the clamping force of the R-bar reached the force corresponding to the yield strain of the R-bar. After adhesion failure, the shear load was carried by the shear pocket system (R-bar and grout in the shear pocket), which acted like a shear key. There is a possibility that cracks formed in the shear pocket system. However, the influence of these cracks on the performance was less than the influence of the loss of adhesion because the shear connector continued to provide a clamping force. After peak load and the breakdown of the shear key action or loss of friction, the shear resistance dropped, resulting in significant slip. The sustained load indicates that the shear force was provided by the strain hardening of shear connector.

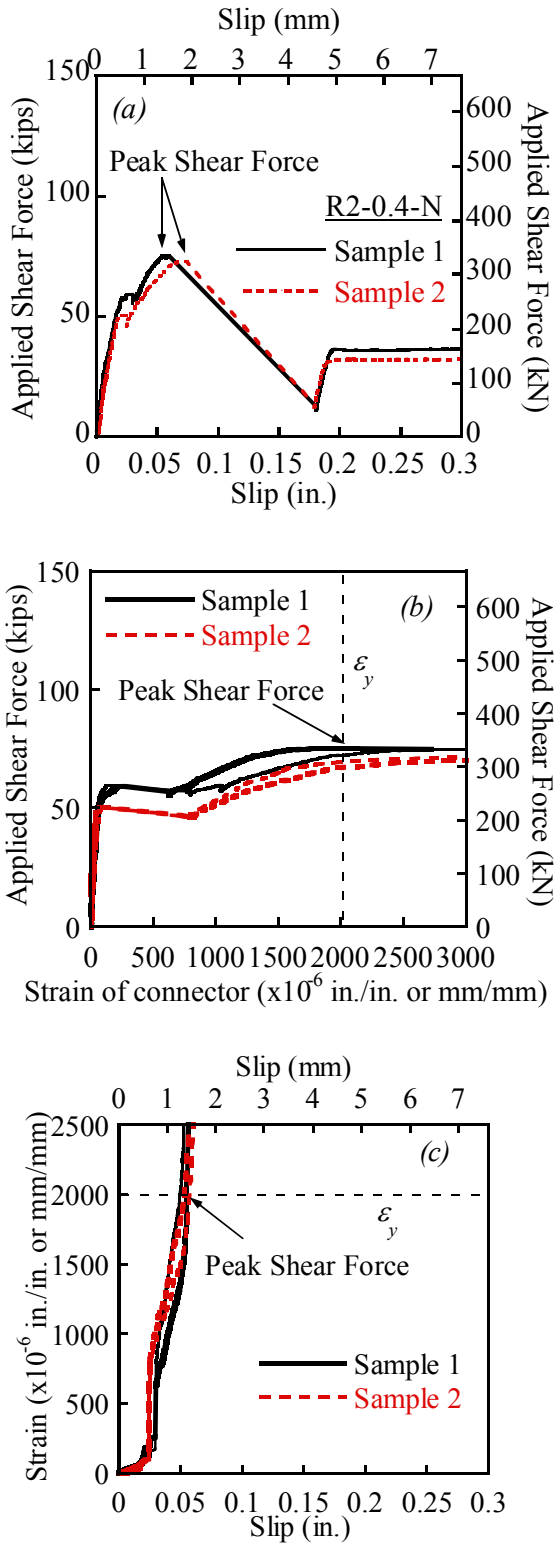

Figure 4-4. Shear load versus slip of R-bar system: (a) Shear force versus slip, (b) Shear force versus strain, (c) Strain versus slip

4.4. FAILURE MECHANISMS IN S2 SERIES PUSH-OFF SAMPLES

The roughened surface on the girder provided relatively strong adhesion between the girder and the haunch of a push-off sample. However, the unroughened surface underneath the precast deck exhibited weak adhesion with the haunch. After adhesion loss, the main source of shear resistance was believed to be provided by the shear pocket system until the peak load.

It is believed that the sustained shear resistance was achieved mainly due to the contribution from the dowel action of the shear connectors. Diagonal shear cracks in the haunch region developed due to flexural deformations of the shear connectors as observed during testing. When high strength shear connectors/couplers were used, the flexural and shear strength of the shear connectors contributed to the dowel action. As the stiffness of the shear connectors increased, the flexural and shear strength mechanisms seemed to be dominant. When the bearing force on the concrete and grout in a shear pocket was lower than the dowel action force, the grout and concrete in the shear pocket was fractured, as shown in Figure 4-5(a). This failure mode was observed with the 1.25-in. (32 mm) diameter shear connector systems in S2-1.83-N and S2-1.83-IO series samples. When the bearing force on the concrete and grout in a shear pocket was higher than the dowel action force, the shear failure of the shear connectors occurred. This failure mode was observed in the 0.75-in. (19 mm) diameter shear connector systems, as shown in Figure 4-5(b).

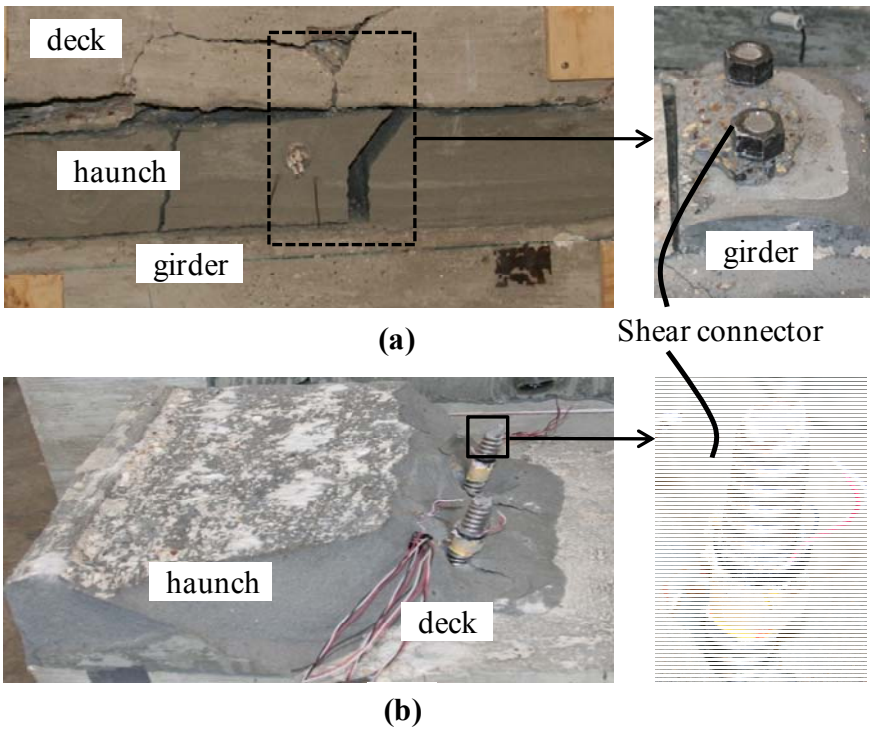

Figure 4-5. Shear connector failure modes: (a) Anchorage failure, (b) Shear connector failure at shear

To achieve a high sustained load and a ductile failure mechanism, the anchorage zone of both the shear pocket and the girder should be sufficiently confined. The effect of different confinement systems on the shear transfer performance in the S2-0.62 and S2-1.83 series samples were studied. Figure 4-6 shows peak and sustained shear loads of the two shear connector/coupler systems with and without confinement. Shear pocket systems with no confinement (i.e., S2-0.62-N and S2-1.83-N series samples) were used as the reference for the comparisons with the confined systems and these were identified as the benchmarks. Maximum values among three replicates were used as the benchmark (hatched columns in Figure 4-6). To assess the effect of confinement on shear transfer mechanisms, using the maximum value as the benchmark was more conservative than taking the average value as the benchmark, and this was done here.

For the 0.75-in. (19 mm) diameter shear connector/coupler system, providing the confinement system did not improve the shear transfer performance (See Figure 4-6 [a]). The O-type confinement (i.e., in S2-0.62-O series samples) resulted in a reduction of the sustained

shear load by approximately 30 percent when compared to the benchmark. When I-type confinement was provided (i.e., in S2-0.62-I series samples), only one sample exhibited higher peak and sustained shear loads than the corresponding benchmark value. When IO-type confinement was provided (i.e., in S2-0.62-IO series samples), the peak shear loads were 11 to 19 percent higher than the benchmark values.

In summary, the hoop confinement (i.e., #3 [M10] reinforcement hoops) did not significantly improve the shear transfer performance of the shear pocket systems with 0.75-in. (19 mm) diameter shear connector/couplers. However, providing IO confinement around the 1.25-in. (32 mm) diameter shear connector/coupler system increased the peak shear resistance by less than 20 percent of the benchmark value (See Figure 4.6 [b]). However, the anchorage failure could not be prevented by the IO confinement system and this resulted in low sustained shear resistance. This indicates that the shear transfer mechanism of the small diameter shear connectors/coupler systems was likely to be different from that of large diameter shear connectors/coupler systems.

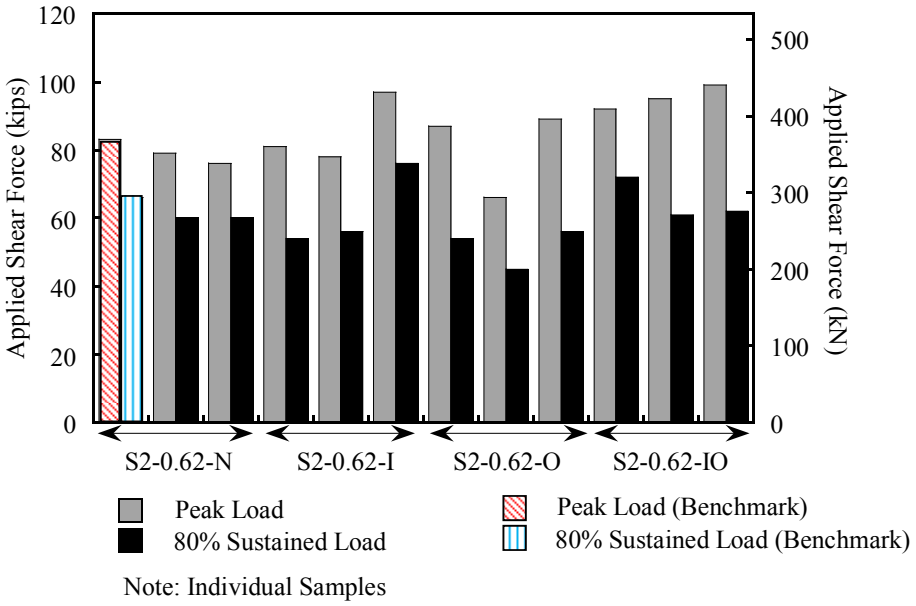

(a)

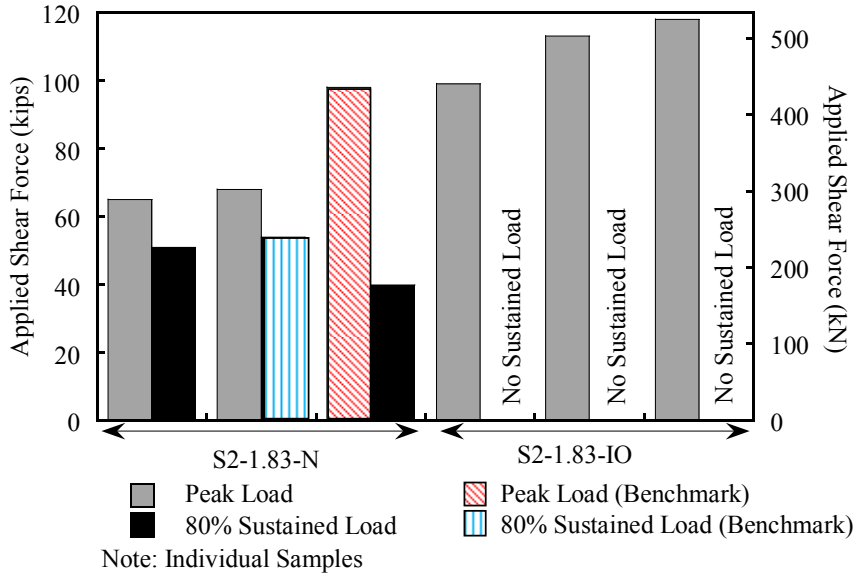

(b)

Figure 4-6. Effect of confinement: (a) 0.75-in. (19 mm) diameter shear connectors/couplers, (b) 1.25-in. (32 mm) diameter shear connectors/couplers

4.5. FAILURE MECHANISMS IN S4 SERIES PUSH-OFF SAMPLES

The S4-3.66-O[H] samples had four shear connectors confined by the HSS tube. Shear connectors failed in two samples, as shown in Figure 4-7(a). One sample experienced the adhesion loss between the surface of the HSS steel tube and the precast deck panel, as shown in Figure 4-7(b). However, there was no sign of shear connector failure in this particular sample. This test was stopped due to the uplift of the deck. The probability of this type of failure in the field would be expected to be low because multiple shear pockets provide additional shear keys and the self-weight of the system provides additional resistance to the uplift. However, holes in the HSS or welded studs on the sides could likely prevent this.

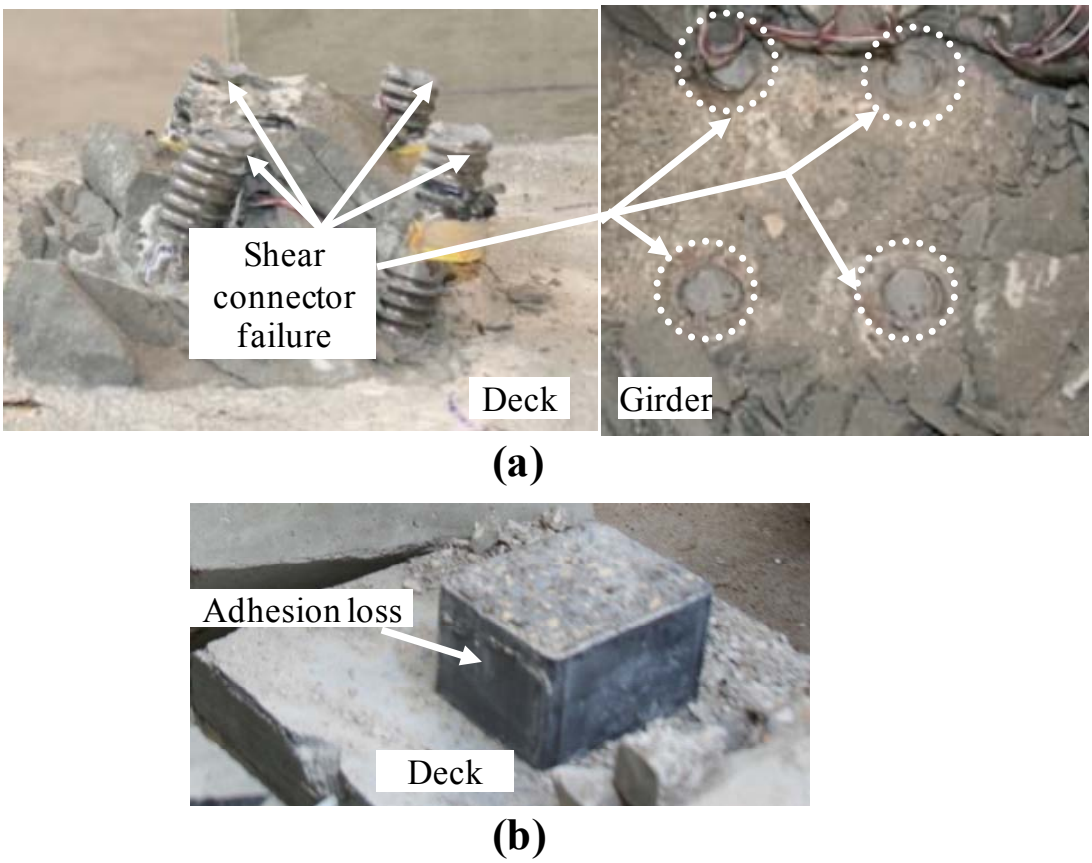

Figure 4-7. Failure modes in S4-3.66-O[H] samples: (a) Shear failure at the interface between shear connector and coupler, (b) Adhesion loss between shear pocket and deck

Figure 4-8 shows the overall comparison of the R-bar system (benchmark), the IO-type confinement system, and the HSS tube system. This figure provides information on the effect of

confinement. Test results indicate that the IO-type confinement with #3 [M10] hoops seemed to be only effective when using 0.75-in. (19 mm) diameter shear connectors. The HSS tube system seemed to provide both shear key and dowel action, resulting in higher peak and sustained loads.

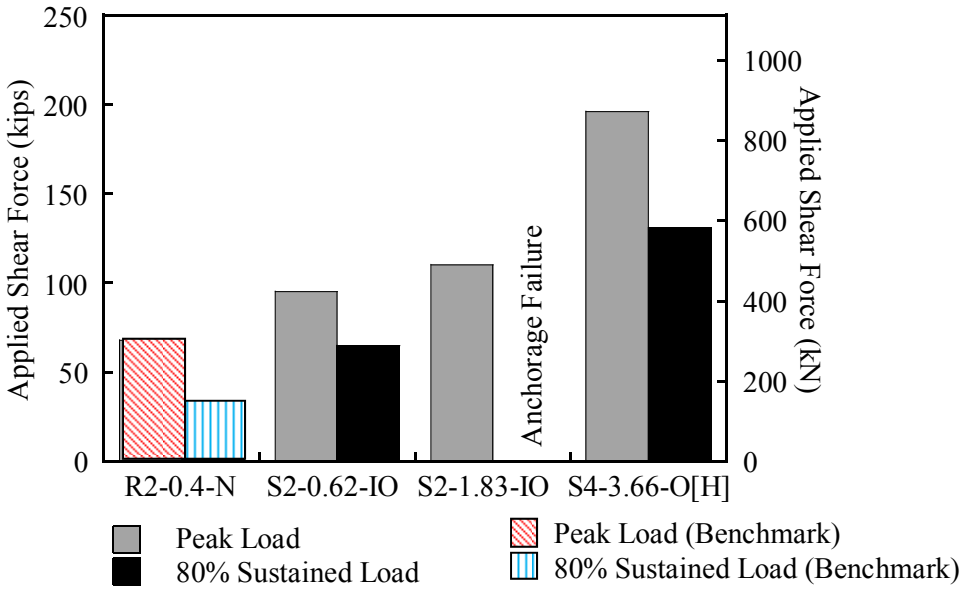

Note: S4-3.66-O[H] 80% sustained load data is average of two samples.
All others are average of three samples.

Figure 4-8. Effect of confinement on shear transfer

4.6. ANALYSIS OF RESULTS

4.6.1. General

Shear friction factors were determined based on the test results, and the number of shear pockets per panel was estimated. The R-bar system achieved the yielding of the R-bars. However, the test results indicate that the shear connector/coupler system did not yield. Design equations in ACI 318-08 (2008) and AASHTO LRFD (2007) were used to estimate the shear transfer capacity of two elements (i.e., girder-CIP deck system with no haunch and shear pockets). It should be noted that the girder-haunch-deck system was not the same system as the girder-CIP deck system or steel girder-precast deck systems. Therefore, a new design approach was necessary to improve the shear transfer mechanism of the shear connector/coupler system.

Figure 4-9 shows three equations that can be used to predict the adhesion loss, peak, and sustained shear loads of the systems tested. For the shear connector/coupler system design, the loss, peak, and sustained loads can be expressed as follows:

$$V_{loss} = cA_{cv} = c'A'_{cv} \quad \text{.....}(a)$$

$$V_{peak} = c'A'_{cv} + \mu_p(\sum A_{sc} \cdot f_y + P_n) \quad \text{.....}(b) \qquad (4.1)$$

$$V_{sus} = \mu_r(\sum A_{sc} \cdot f_y + P_n) \quad \text{.....}(c)$$

where:

- V_{loss} is the shear force at the adhesion loss,
- V_{peak} is the peak shear force,
- V_{sus} is the sustained or post-peak force,
- c is the adhesion stress on the interface between girder and deck,
- A_{cv} is the effective interface area of concrete engaged in shear transfer (haunch and deck contact area),
- c' is the interlock of the crack surface in the shear pocket system,
- A'_{cv} is the effective interface area of the concrete engaged in shear transfer (herein referred to as the cracked area in the shear pocket system),
- A_{sc} is the cross-sectional area of shear connectors,
- f_y is the yield strength of the shear connector,
- μ_p is the coefficient of friction at peak shear force for surfaces roughened to an amplitude of approximately 0.20 to 0.25 in. (5 to 6.4 mm),
- μ_r is the coefficient of friction at sustained force (herein 80 percent V_{sus}) for surfaces roughened to an amplitude of approximately 0.20 to 0.25 in. (5 to 6.4 mm), and
- P_n is a permanent normal force to the shear plane.

At the point of adhesion loss, the adhesion load (cA_{cv} in Eq. (4.1)(a)) was transferred to the shear pocket system ($c'A'_{cv}$ in the first term of Eq. (4.1)(b)). It was assumed that this load

could be transferred to the shear key when the shear connectors are in tension. The slip at the peak load was relatively small compared to the slip during the sustained load region. The second term of Eq. (4.1)(b) was the shear key action provided by the clamping force at the peak shear load. Eq. (4.1)(c) includes f_y multiplied by the coefficient, μ_r to estimate the shear capacity of the bars resulting from shear failure. In the following section, the coefficients are determined from the test results.

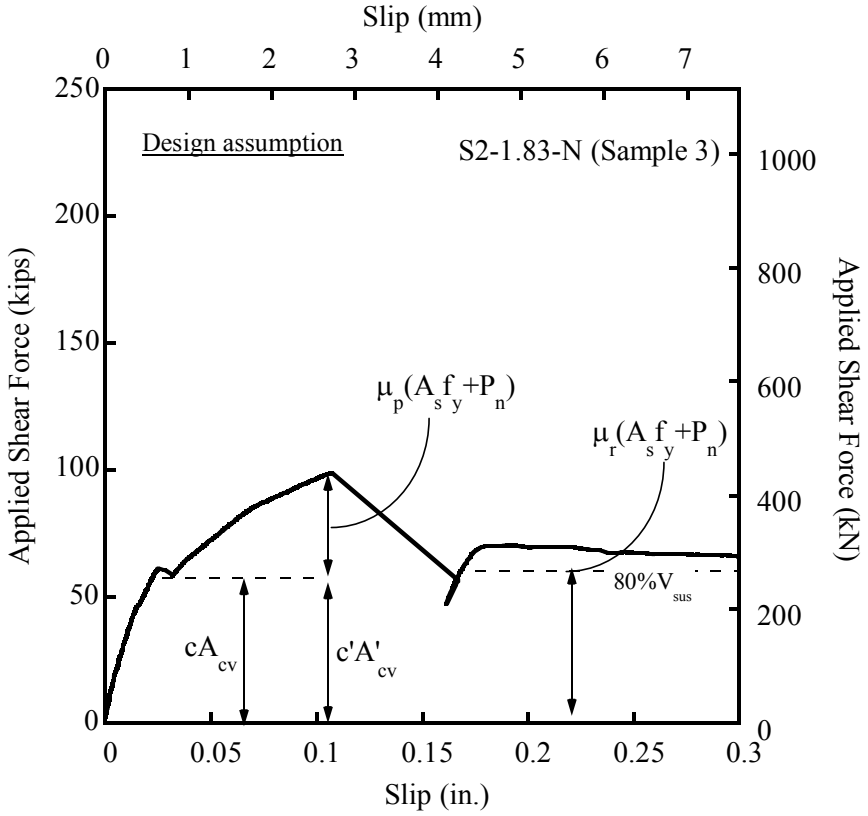

Figure 4-9. Three equations of shear transfer mechanisms

4.6.2. Determination of Shear Transfer Parameters

Table 4-2 summarizes the coefficients along with the failure mode and the stress levels of the shear connectors. The average of the *c* values from all the samples was 127 psi (875 kN/m^2) and the standard deviation was 15 psi (103 kN/m^2). These consistent values indicate that the adhesion capacity was not dependent on the shear connector type. The 0.75-in. (19 mm) diameter shear connector and the conventional R-bar system provided higher *c′* values than the

1.25-in. (32 mm) diameter shear connector system, except when the HSS tube confinement system was used. For 1.25-in. (32 mm) diameter shear connector/coupler systems, the IO-type confinement increased the shear key action. However, there was no significant increase in the shear capacity of the 0.75-in. (19 mm) diameter shear connector/coupler system. The tensile strength of the shear connector influenced the normal displacement at the girder-haunch-deck interface, which in turn influenced the roughness of the interface. This could change the coefficient of friction between the girder-haunch-deck during slipping. As the stiffness of the shear connector decreased, the coefficient of friction values at peak and the sustained shear force increased, indicating the high clamping stress in the shear connectors. While the R2-0.4-N samples had the highest average values for the coefficient of friction at peak and sustained shear force, the S2-1.83 series samples exhibited the lowest values (or no data were available when anchorage failure occurred).

Table 4-2. Summary of shear transfer parameters

Series I.D.	Sample number	$A_s f_y + P_n$, kips	$c'A'_{cv}$ or cA_{cv}, kips	c, psi	c', psi	μ_p	μ_r (80 percent V_{sus})	Bar failure mode
R2-0.4-N	1	27	-	-	-	-	1.21	Tension failure
	2	27	52	125	1839	0.84	1.29	
	3	27	50	120	1768	0.84	1.26	
	Average	27	51	123	1804	0.84	1.25	
S2-0.62-N	1	70	63	152	1264	0.28	0.96	Shear failure
	2	70	54	130	1084	0.36	0.86	
	3	70	50	120	1000	0.37	0.86	
	Average	70	56	134	1116	0.34	0.89	
S2-0.62-I	1	70	54	130	1080	0.39	0.77	Shear failure
	2	70	54	130	1080	0.35	0.81	
	3	70	55	132	1100	0.60	1.09	
	Average	70	54	131	1087	0.45	0.89	
S2-0.62-O	1	70	48	115	960	0.56	0.78	Shear failure
	2	70	45	108	900	0.30	0.64	
	3	70	62	149	1240	0.39	0.81	
	Average	70	52	124	1033	0.42	0.74	
S2-0.62-IO	1	70	49	118	980	0.62	1.04	Shear failure
	2	70	67	162	1348	0.40	0.87	
	3	70	61	147	1222	0.55	0.89	
	Average	70	59	142	1183	0.52	0.93	
S2-1.83-N	1	179	45	109	568	0.11	0.29	-
	2	179	42	101	526	0.14	0.30	
	3	179	45	109	568	0.29	0.22	
	Average	179	44	106	554	0.18	0.27	
S2-1.83-IO	1	179	61	147	763	0.21	-	*8 percent f_u
	2	179	58	139	725	0.31	-	*5 percent f_u
	3	179	-	-	-	-	-	-
	Average	179	60	143	744	0.26	-	-
S4-3.66-O[H]	1	356	-	-	-	-	-	*13percent f_u
	2	356	78	112	975	0.31	0.33	shear
	3	356	86	124	1075	0.28	0.41	shear
	Average	356	82	118	1025	0.30	0.37	-

Note: * indicates percent stress of ultimate capacity of a shear connector; '-' indicates no data available;1 psi = 6.895 MPa; 1 kip = 4.448 kN

4.6.3. Shear Demand Estimation

Table 3.4.1-1 of AASHTO LRFD (2007) provides the following load combination for STRENGTH-I limit state:

$$Q = 1.25DC + 1.5DW + 1.75(LL + IM) \tag{4.2}$$

where:

- Q is the factored load effect (herein V_u),
- DC is the dead load effect without the wearing surface weight,
- DW is the dead load effect due to wearing surface weight,
- LL is live load, and IM is dynamic load.

The maximum live load can be estimated based on the combination (HL-93 loading condition) of HS20 truck design load and design lane load. The dynamic load effect factor can be taken as 1.33. Therefore, $LL+IM$ is equal to 1.33 LL. For this case, the number of girders will be assumed to be 6. The bearing weight is estimated to be 0.109 kips/ft/girder (1.59 kN/m/girder). The barrier weight is assumed to be 326 lb/ft (4.75 kN/m). The weight of 1.5-in. (38 mm) thick wearing surface is assumed to be 0.0175 kips/ft^2 (0.84 kN/m^2). The clear roadway width is assumed to be 6 ft per girder. This leads to the wearing surface weight of 0.105 kips/ft^2 (5.027 kN/m^2). The effective depth will be taken as 0.72 h. Table 4-3 shows the demand shear transfer force at the critical section for shear (the first panel from the support). The dimensions of the girders are presented in Figure 4-10 through Figure 4-12.

Note that these demand loads were calculated based on the 2007 AASHTO LRFD and TxDOT I-girder with varied span lengths. They are different from the demand load (based on one girder type with the older types of TxDOT girders) reported in 0-6100-1 and 0-6100-2, and are likely more realistic of current TxDOT design practices.

Table 4-3. Demand of shear transfer force (V_h)

Beam Type	Top flange width, b_f, inch (mm)	Structure Depth, h *, inch (mm)	Max. Span length, ft (m)	V_u (Strength limit I), kips (kN)	V_h, kips/inch (kN/m)
Tx28	36 (914)	40 (1016)	80 (24)	109 (485)	4.2 (0.74)
Tx34	36 (914)	46 (1168)	95 (29)	119 (529)	4.0 (0.70)
Tx40	36 (914)	52 (1321)	105 (32)	121(538)	3.6 (0.63)
Tx46	36 (914)	58 (1473)	120 (37)	130 (578)	3.5 (0.61)
Tx54	36 (914)	66 (1676)	140 (43)	140 (623)	3.2 (0.56)
Tx62	42 (1067)	74 (1880)	150 (46)	139 (618)	2.9 (0.51)
Tx70	42 (1067)	82 (2083)	150 (46)	127 (565)	2.4 (0.42)

Note:* h = Beam depth + Precast deck depth (8 in.) + Haunch (4 in.).

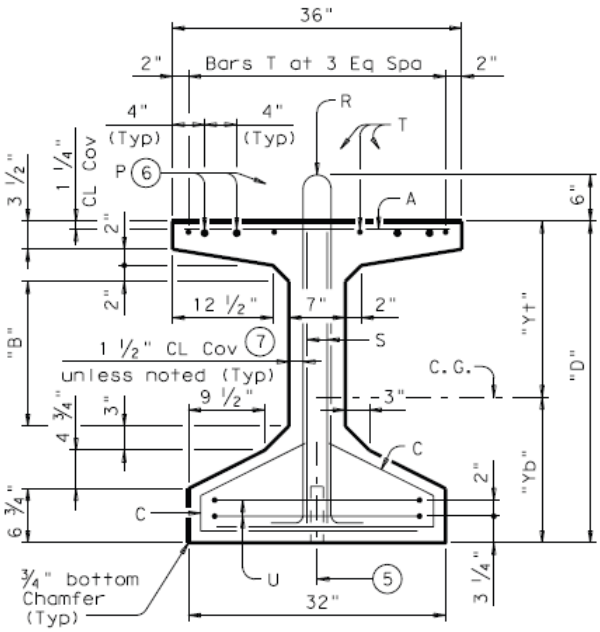

TYPE Tx28, Tx34 & Tx40

GIRDER DIMENSIONS AND SECTION PROPERTIES

Girder Type	"D" (in.)	"B" (in.)	"Y+" (in.)	"Yb" (in.)	Area ($in.^2$)	"Ix" ($in.^4$)	"Iy" ($in.^4$)	Weight (plf)
Tx28	28	6	15.02	12.98	585	52,772	40,559	610
Tx34	34	12	18.49	15.51	627	88,355	40,731	653
Tx40	40	18	21.90	18.10	669	134,990	40,902	697

Figure 4-10. TxDOT I-Girder (Tx28, Tx34, and Tx40) (http://www.txdot.state.tx.us)

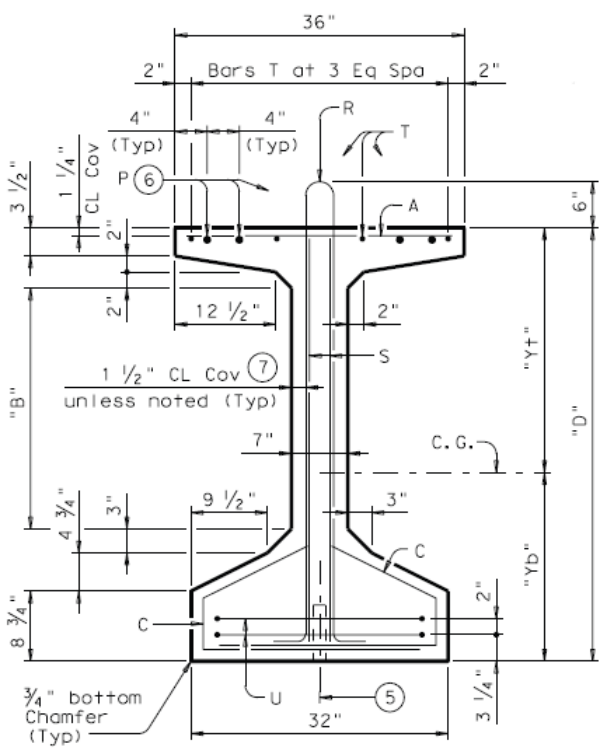

TYPE Tx46 & Tx54

GIRDER DIMENSIONS AND SECTION PROPERTIES

Girder Type	"D" (in.)	"B" (in.)	"Yt" (in.)	"Yb" (in.)	Area ($in.^2$)	"Ix" ($in.^4$)	"Iy" ($in.^4$)	Weight (plf)
Tx46	46	22	25.90	20.10	761	198,089	46,478	793
Tx54	54	30	30.49	23.51	817	299,740	46,707	851

Figure 4-11. TxDOT I-Girder (Tx46 and Tx54) (http://www.txdot.state.tx.us)

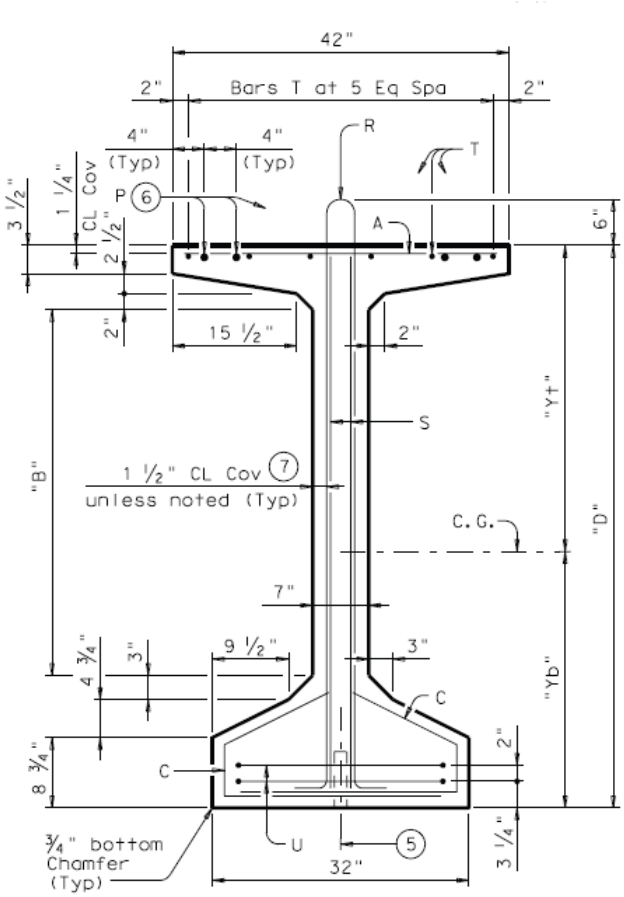

TYPE Tx62 & Tx70

GIRDER DIMENSIONS AND SECTION PROPERTIES

Girder Type	"D" (in.)	"B" (in.)	"Yt" (in.)	"Yb" (in.)	Area ($in.^2$)	"Ix" ($in.^4$)	"Iy" ($in.^4$)	Weight (plf)
Tx62	62	37 1/2"	33.72	28.28	910	463,072	57,351	948
Tx70	70	45 1/2"	38.09	31.91	966	628,747	57,579	1,006

Figure 4-12. TxDOT I-Girder (Tx62 and Tx70) (http://www.txdot.state.tx.us)

4.6.4. Shear Pocket Design

The smaller of the peak load and sustained load can be taken as the nominal shear transfer capacity and this can be used to determine the number of shear pockets in a precast overhang panel. The nominal shear transfer capacity of all shear pockets per panel can be estimated using the following equation:

$$\min \begin{cases} V_{peak} = c' \cdot n \cdot A'_{cv} + \mu_P \cdot (\sum A_{sc} \cdot f_y) \cdot n \\ V_{sus} = \mu_r (A_s f_y + P_n) \cdot n \end{cases} \quad (4.3)$$

where the terms were defined earlier and n is the number of pockets per overhang panel. Using Eq. (4.3) and the AASHTO demand load information provided, the required number of pockets for the different shear connector/coupler systems can be determined. The capacity of the shear connector/coupler systems must exceed the shear demand of each panel at the end of the girder, and this was calculated and is shown in Table 4-4. In all the cases, V_{sus} was found to be less than V_{peak} (as shown in Eq. 4.3). The required number of shear pockets varied from two to eight. For the design of a Tx28 girder with an 8-ft (2.43 m) long precast panel, it is recommended that three shear pockets with four 1.25-in. (32 mm) diameter shear connectors in each pocket confined with HSS steel tube be used. It should be noted that a cost analysis was not performed but adding the steel tubing system will likely increase costs.

Table 4-4. Estimated shear pockets for AASHTO LRFD demands

Girder Type	Span, ft (m)	Required V_n /panel, kips (kN)	#4 R-bar shear connector*	0.75-in. diameter shear connector		1.25-in. diameter shear connector	
			2 x R2-0.4-N	S2-0.62-N	S2-0.62-IO	S2-1.83-N	S4-3.66-O[H]
Tx28	80 (24)	403 (1793)	7	7	6	8	3
Tx34	95 (29)	384 (1708)	6	6	6	8	3
Tx40	105 (32)	346 (1539)	6	6	5	7	3
Tx46	120 (37)	336 (1495)	6	6	5	7	3
Tx54	140 (43)	307 (1366)	5	5	5	6	2
Tx62	150 (46)	278 (1237)	5	5	4	6	2
Tx70	150 (46)	230 (1023)	4	3	3	4	2

Note: *It was assumed that two R-bar shear connectors (i.e., 4 legs) are placed within a pocket.

4.7. SUMMARY

This section provides the information on the overall findings in the push-off tests.

- There were five stages of shear transfer and failure mechanisms prior to system failure. These stages included the initial adhesion loss, shear key action, shear key action failure, dowel action of the shear connectors at the sustained load, and final failure of the system.

- The roughened surface on the girder surface provided a stronger adhesion between the haunch material and the adjacent girder surface in the push-off samples (i.e., V_{loss} values). However, V_{loss} values were not used to design the connections. Shear key action clamped by shear connectors increased the interface shear capacity until the shear key failed. Dowel action of the shear connectors is likely the main source of the interface shear capacity after shear key failure.

- Four confinement systems were tested. These included three different hoop confinement systems (inner, outer, and both) and one steel tube system. Test results indicate that the steel tube system provided both improved shear key action and improved dowel action and resulted in higher peak and sustained shear loads. It was found that neither the inner confinement system alone or the outer confinement system alone improved the confinement significantly. The S2-0.62-IO series (containing inner and outer confinement) seemed to be effective only when the 0.75-in. (19 mm) diameter shear connector/coupler system was used.

- A new design equation (Eq. 4.3) is proposed to estimate the shear capacity of the girder-haunch-deck systems. The smaller value of the peak and sustained shear capacity can be taken as the nominal shear transfer capacity and this can be used to determine the number of shear pockets in a panel. Using the sustained shear value may be conservative – using a percentage (less than 100 percent) of the peak load will likely result in a lower number of pockets but may not be as conservative. The number of shear pockets in each panel was determined for the newer TxDOT girder-

haunch-deck systems. Based on 80 percent of the sustained load, results indicate that three shear pockets with four 1.25-in. (32 mm) diameter shear connectors in each pocket, with each pocket confined with HSS steel tube is sufficient for Tx28 girder-haunch-deck systems when using the AASHTO LRFD demand.

5. SUMMARY, CONCLUSIONS, AND RECOMMENDATIONS

5.1. SUMMARY AND CONCLUSIONS

The implementation of full-depth, precast overhang panel systems have the potential to improve constructability and make bridges more economical. Initial testing and analyses reported in 0-6100-2 resulted in a design that required a large number of shear pockets in the overhang panels to achieve the required interface shear capacity. Report 0-6100-1 took a different approach for the design of the shear pockets and reported that the number of pockets per panel could be reduced. However, this analysis included only one beam type and one span. In addition, the demand was less than that typically used by AASHTO and the analysis was performed for older types of TxDOT precast beams. The testing and analyses documented in this report provide an assessment for determining the number of shear pockets required for various connector systems for the newer TxDOT beams and recommendations are provided for a number of beam types and spans. Specifically, this research was performed to assess a new shear connector system for a full-depth precast deck to provide sufficient safety and structural integrity. A total of 24 push-off tests were performed to investigate the shear transfer performance. Test results were used to develop an appropriate equation for the design of high strength shear connector/coupler systems for girder-haunch-deck systems. The major findings are presented as follows:

1. *Mechanisms:* For the shear connector/coupler systems documented in this report, there were five distinct stages up to failure. These stages included the initial adhesion loss, shear key action, shear key action failure, dowel action of the shear connectors at the sustained load, and final failure of the system.

2. *Mechanisms:* The roughened surface on the girder surface provided a stronger adhesion between the haunch material and the adjacent girder surface in the push-off samples. The unroughened surface on the underside of the precast deck panel exhibited weaker adhesion to the haunch material. Surface roughening improves the adhesion of the system but the surface adhesion (V_{loss}) was not used in

determining the shear resistance of the interface plane. After adhesion loss, the main source of shear resistance was provided by shear key action near the shear pocket (shear connectors/couplers, filling materials, and a confinement system) until the peak load was achieved. The sustained load seems to be a result of the dowel action of shear connectors.

3. *Confinement Effect:* Test result indicated the #3 [M10] hoop confinement system (S2-0.62-IO) seemed to be effective only when the 0.75-in. (19 mm) diameter shear connector/coupler system was used. The steel tube system provided both improved shear key action and dowel action and resulted in higher peak and sustained shear loads.

4. *Design:* This research resulted in the development of a new design equation for estimating the shear capacity of girder-haunch-deck systems. Based on this proposed equation, results indicate that pockets containing 1.25-in. (32 mm) diameter shear connectors with steel tube confinement require the least number of pockets. Note that the design uses 80 percent of the sustained load (V_{sus}). This may be conservative. Using a percentage less than 100 and the peak load (V_{peak}) may result in even further reductions in pockets and connectors. For Tx 28 girders (girders with the highest demand), results indicate that three shear pockets are required for end panels. Table 4-4 provides a summary for different girder types and connector systems. It should be noted that the research in this report only assessed the shear capacity of systems with single pockets under lab conditions. Issues related to fatigue, incorrect construction, non-uniform stress distributions, and other potential influencing variables were not assessed. Care and good engineering judgment should be used when designing overhang panels with the proposed equation.

5.2. RECOMMENDATIONS

The following recommendations and future work are recommended based on the findings from this project.

1. The research findings indicate that high strength shear connectors with an appropriate confinement system can reduce the number of shear pockets required in precast overhang panels.

2. TxDOT should use appropriate friction factors and cohesion factors considering the diameter of the shear connectors and the effectiveness of confinement. When large diameter shear connectors are proposed, the friction factor should be reduced. When a confinement system is proposed, the cohesion factor can be increased. However, the cohesion factor should be limited to achieve sustained ductile behavior. The design should be executed to the bar failure mode without deck and shear pocket failure.

3. The grouping effects of the shear connectors in pockets should be further investigated for both R-bar systems and shear connector systems. Additional testing containing two shear connectors confined by the steel tube would be beneficial to assess grouping effects.

4. To prevent interfacial failure between the steel confining tube and the deck concrete, holes should be cut into the steel tube or protrusions should be welded to the outside surface of the tube. This will likely resist slip in the vertical direction.

5. The full-scale tests with multiple shear pockets are necessary to verify proposed design equation.

REFERENCES

AASHTO LRFD (2007). *AASHTO LRFD Bridge Design Specifications*, 4th Edition, 2007, American Association of State Highway and Transportation Officials, Washington, D.C.

ACI (2008). Building Code Requirements for Reinforced Structural Concrete (ACI 318-08) and Commentary, American Concrete Institute, Farmington Hills, Detroit.

Araujo, D. L., and Debs, M. K. El. (2005). "Strength of Shear Connection in Composite Bridges with Precast Decks Using High Performance Concrete and Shear-keys, Materials and Structures, Vol. 38, pp. 173-181.

ASTM A615 (2008). "Standard Specification for Deformed and Plain Carbon-steel Bars for Concrete Reinforcement." Annual book of ASTM standards, The American Society for Testing and Materials, West Conshohocken, Pennsylvania.

ASTM C39 (2007). "Standard Test Method for Compressive Strength of Cylindrical Concrete Specimens." Annual book of ASTM standards, The American Society for Testing and Materials, West Conshohocken, Pennsylvania.

ASTM C109 (2008). "Standard Test Method for Compressive Strength of Hydraulic Cement Mortars (Using 2-in or [50mm] Cube Specimens)." Annual book of ASTM standards, The American Society for Testing and Materials, West Conshohocken, Pennsylvania.

ASTM C1170 (2007). "Standard Specification for Packaged Dry, Hydraulic-Cement Grout." Annual book of ASTM standards, The American Society for Testing and Materials, West Conshohocken, Pennsylvania.

Birkeland and Birkeland (1966). "Connections in Pre-Cast Concrete Construction." ACI Journal, Vol. 63, No. 3, pp. 345-367.

Coulomb, C. A. (1776). *Essai sur une application des regles des maximis et minimis a quelquels problems de statique, relatifs a la architecture.*Academie Royale des Sciences,, Vol. 7, pp. 343-382.

Kovach, J. D., and Natio, C. (2008). "Horizontal Shear Capacity of Composite Concrete Beams without Interface Ties." Advanced Technology for Large Structural Systems (ATLSS) Report No. 08-05, Lehigh University, Bethlehem.

Mattock, A. H., and Hawkins, N. M. (1972). "Shear Transfer in Reinforced Concrete–Recent Research," Precast/Prestressed Concrete Institute (PCI) Journal, Vol. 17, No. 2, pp. 55-75.

Mattock, A. H., Li, W. K., and Want, T. C. (1976). "Shear Transfer in Lightweight Reinforced Concrete," PCI Journal, Vol. 21, No. 1, pp. 20-39.

Mattock, A. H. (1974). "Shear Transfer in Concrete Having Reinforcement at an Angle to Shear Plane," Shear in Reinforced Concrete, SP-42, American Concrete Institute, Farmington Hills, MI, pp. 17-42.

Mattock, A. H. (2001). "Shear Friction and High-Strength Concrete," ACI Structural Journal, Vol. 98, No. 1, pp. 50-59.

NCHRP Report 584 (2008). "Full-Depth Precast Concrete Bridge Deck Panel System." Transportation Research Board, Washington, D.C.

PCI Design Handbook (2004). Precast and Prestressed Concrete, 6th Edition, MNL-120-4, Precast/Prestressed Concrete Institute, Chicago, IL, p. 736.

Patton, F. D. (1966). "Multiple mode of shear failure in rock and related materials," PhD Dissertation, University of Illinois at Urbana-Champaign, IL,

Park, P., and T. Paulay (1975). *Reinforced Concrete Structures*, John Wiley & Sons, New York, p. 769.

Rezansoff, T., and Hosain, M. U. (1983). "Headed Shear Stud Connectors in a Stub-girder floor system: a preliminary study: Reply," Canadian Journal of Civil Engineering.

Scholz, D.P., Wallenfelsz, J. A., Lijeron, C., and Roberts-Wollmann, C.L. (2007). "Recommendations for the Connection Between Full-Depth Precast Bridge Deck Panel Systems and Precast I-Beams." Report No. VTRC 07-CR17, Virgnia Transportation Research Council, Charlottesville, VA.

Sullivan, S. (2007). "Construction and Behavior of Precast Bridge Deck Panel Systems." Ph.D. Dissertation, Virginia Tech, Blacksburg.

Trejo, D., Hite, M., Mander, J., Mander, T. J., Henley, M., Scott, R., Ley, T., and Patil, S. (2009). "Development of a Precast Bridge Deck Overhang." TxDOT Report 0-6100-2.

Trejo, D., Hite, M., Mander, J., Mander, T. J., Henley, M., Scott, R., Ley, T., and Patil, S. (2011). "Development of a Precast Bridge Deck Overhang." TxDOT Report 0-6100-1.